

Chapter 12

Remote Detection of Invasive Alien Species



Erik A. Bolch, Maria J. Santos, Christiana Ade, Shruti Khanna,
Nicholas T. Basinger, Martin O. Reader, and Erin L. Hestir

12.1 Introduction

Invasive alien species (IAS) are non-native species with a rapid spread potential that can have negative ecological, environmental, and economic effects on the environments where they have been introduced (Masters and Norgrove 2010). The current rate and variety of species invasions is unprecedented in the fossil record (Ricciardi 2007). Global rates of invasion increased from around 8 records per year in 1800 to 1.5 per day in 1996. Although this rate may be partly the result of better record keeping, the rate is consistent across most taxa and shows little sign of slowing down (Seebens et al. 2017). Driven by climate change, invasion is expected to continue apace as global temperatures continue to rise and human societies and economies become increasingly connected around the world (Penk et al. 2016; van Kleunen et al. 2015).

E. A. Bolch (✉) · C. Ade · E. L. Hestir
University of California Merced, School of Engineering, Environmental Systems,
Merced, CA, USA
e-mail: ebolch@ucmerced.edu; cade@ucmerced.edu; ehestir@ucmerced.edu

M. J. Santos · M. O. Reader
University of Zürich, Department of Geography and University Research Priority Program in
Global Change and Biodiversity, Zürich, Switzerland
e-mail: maria.j.santos@geo.uzh.ch; martin.reader@geo.uzh.ch

S. Khanna
University of California Davis, Department of Land, Air, and Water Resources,
Davis, CA, USA
e-mail: shrkhan@ucdavis.edu

N. T. Basinger
University of Georgia, Department of Crop and Soil Sciences, Athens, GA, USA
e-mail: nicholas.basinger@uga.edu

12.1.1 Invasive Alien Species and Global Environmental Change

Human-mediated IAS introductions, deliberate or unintentional, tend to be much faster than natural processes (e.g., wind, animal; Theoharides and Dukes 2007; Hulme 2009; Pyšek et al. 2009; Seebens et al. 2017). Invasion pathways differ between taxa; intentional transport (escape and release) is most important for plants and vertebrates, while unintentional transport is more significant for invertebrates, algae, and microorganisms (Saul et al. 2017). Roads, tracks, and waterways create natural and artificial corridors for invasion, exposing ecosystems to invasion, particularly in emerging economies where development is rapid (Mortensen et al. 2009; Masters and Norgrove 2010). Globally, the continued expansion of tourism, air transport, and trade is dramatically heightening propagule pressure and subsequent invasion (Hulme 2015).

Global environmental changes, particularly changes in climate and weather patterns, nutrient cycles, and land use, generally drive increasing invasions while also making invasion prevalence, impacts, and feedbacks to the Earth system less predictable (Bradley et al. 2010; Dukes and Mooney 1999). These same change processes can also alter IAS transport and introduction mechanisms, hindering monitoring and control (Hellmann et al. 2008; Walther et al. 2009) and making it more challenging to predict future spread. Moreover, these changes stress ecosystems and increase invasion success (Simberloff 2000). Climate and land use changes drive species range shifts, potentially creating new invasion hotspots (Bellard et al. 2013; Bradley et al. 2010) while decreasing invasion risk and increasing recovery potential in other regions (Allen and Bradley 2016). Thus, observing the geographic patterns of the spread of IAS is critical to understand their origins, pathways, and invasion processes on a changing planet.

12.1.2 Biodiversity Impacts and Global Relevance

Biodiversity provides ecosystems with the capacity to respond to biotic and abiotic conditions and stress, often used as an indicator of ecosystem resilience. IAS threaten biodiversity through competition, hybridization, population reduction, and extinction of native species and modification of habitat. It has been estimated that 42% of all threatened or endangered species are at risk primarily because of IAS (Pimentel et al. 2005). IAS are able to thrive because they arrive in new ecosystems without coevolved local competitors, parasites, and pathogens to regulate their numbers (Keane and Crawley 2002) and are potentially able to exploit resources and niche spaces that natives cannot (Byers and Noonburg 2003; Levine 2000). Hybridization with local organisms reduces genetic diversity and further increases extinction risk (Mooney and Cleland 2001). For example, cheatgrass (*Bromus tectorum*) introduction to the Great Basin in North America resulted in decreases in

biodiversity and dramatic changes in the ecosystem, as cheatgrass eliminated native competing shrubs (and thus species dependent on them) and increased fire frequency in the region (Pimentel et al. 2005). Ecosystem services losses and subsequent economic impacts of IAS are also high, from agriculture, forestry, and fisheries production losses to decreased recreation and tourism revenues (Pimentel et al. 2005). As of 2005, direct costs of invasive species and their management in the United States alone reach around \$120 billion per year, excluding the degradation of invaluable ecosystem services (Pimentel et al. 2005). Globally, costs of invasions and IAS management exceed those of natural disasters by an order of magnitude (Ricciardi et al. 2011).

The increasing economic and ecosystem impacts of IAS require international cooperation given the transboundary nature of IAS transport, spread, and impacts (Fig. 12.1). In recognition of the global threat IAS pose to biodiversity, ecosystems, economies, and livelihoods, the Convention on Biological Diversity (CBD) Aichi Target #9 specifically addresses IAS: “By 2020, invasive alien species and pathways are identified and prioritized, priority species are controlled or eradicated and measures are in place to manage pathways to prevent their introduction and establishment.” The International Union for Conservation of Nature supports Aichi Target #9 through its global network of scientific and policy experts in the Invasive Species Specialist Group (ISSG), maintaining several databases including the Global Invasive Species Database (GISD) and the Global Register of Introduced and Invasive Species (GRIIS). The Intergovernmental Science-Policy Platform on Biodiversity and Ecosystem Services (IPBES) administered by the UN Environment Programme (UNEP) includes Deliverable 3(b)(ii): “Thematic assessment on invasive alien species and their control.” This indicates that IPBES will be assessing IAS status and producing a deliverable directly to policy-makers to assist in preservation of biodiversity and ecosystem services.

IAS-driven disturbances disproportionately affect developing countries, where livelihoods often depend on local natural resources that are threatened if IAS

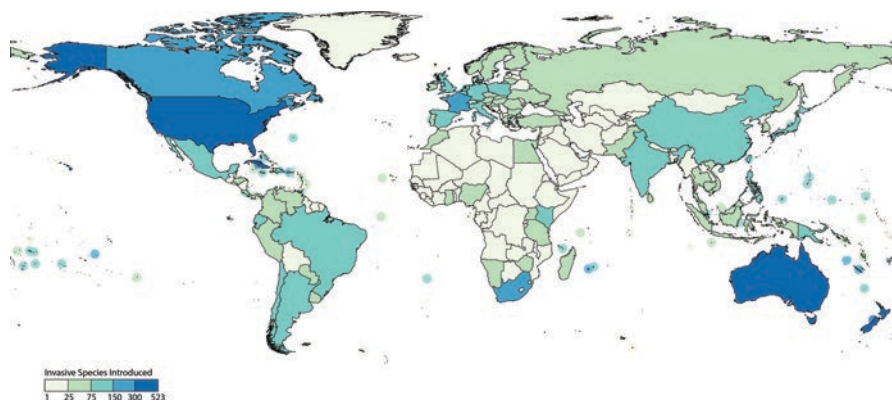


Fig. 12.1 2016 Estimates of global IAS introductions by country from the Global Invasive Species Database (GISD). (Data acquired from Turbelin et al. (2017) for reproduction)

become prevalent (Masters and Norgrove 2010). Therefore, minimizing IAS spread is necessary to meet the targets in UN Sustainable Development Goal 15, *Life on Land*, which has a target focusing specifically on preventing introduction, controlling, and eradicating IAS. The European Environmental Agency (EEA 2012) has also developed an “invasive alien species in Europe” indicator summarizing the trends of invasions since 1900 and the greatest biodiversity threats. Meanwhile the US National Invasive Species Council coordinates and facilitates data interoperability across data providers and users, including defining data standards, formats, and protocols and facilitating cooperation across sectors and governments (National Invasive Species Council 2016).

In order to reduce the pressure of IAS on biodiversity and ecosystems, globally integrated approaches to IAS prioritization, management, and control are needed. Fundamental to international cooperation is cross-border policy and cooperation and transboundary assessments that are implemented within a global monitoring framework (Latombe et al. 2017). Following the Essential Biodiversity Variable (EBV) concept (see Fernández et al., Chap. 18), essential variables for invasion monitoring have recently been proposed by Latombe et al. (2017) to underpin a global monitoring system for IAS. Essential variables for IAS include occurrence, alien status, and alien species impact. Remote sensing (RS) is a valuable observation tool in this new EBV framework because it can be used to identify locations, cover, abundance, biomass, and other traits of IAS. Because it provides synoptic spatial, routine monitoring with fine scale, high-resolution RS can be used to identify sources of IAS and pathways for spread. RS-enabled IAS location data can inform control decisions and, with routine monitoring, can be used to quantify trends and predict invasion processes into the future to support policy decisions and management actions aimed at preventing undesired spread.

12.1.3 Remote Sensing for Detection of Plant Invasions

RS has long been favored as a tool for IAS mapping, specifically for plants, due to its ability to provide synoptic views over large geographical extents. This provides an advantage over field surveys, which are often limited to a small areas and may be in difficult to access locations. Historically, RS has been crucial in IAS detection. As far back as the 1970s, color infrared (IR) photos captured from airplanes were used to target herbicide applications to control water hyacinth (*Eichhornia crassipes*) infestations (Rouse et al. 1975). Over time, the state of the science has progressed substantially. Current technologies such as hyperspectral imaging spectroscopy and light detection and ranging (lidar) make it possible to detect and differentiate plant species within the same functional groups. Coupled with advances in image processing algorithms, these technologies have enabled accurate, repeatable RS measurements over time, providing consistent monitoring records to support control efforts.

Three factors make mapping IAS using RS most viable (He et al. 2015). First, when the IAS is the dominant growth form or has large homogeneous patches, it is easier to train a classifier to recognize it. For example, water hyacinth is sometimes the only IAS in lakes, so mapping it is as easy as separating bright green vegetation from spectrally dark water (Venugopal 2002). This is feasible with simple color IR aerial photography (Rouse et al. 1975) or multispectral satellite data such as that from Satellite Pour l'Observation de la Terre (SPOT) or Landsat. Second, when the target IAS has a unique phenology, it is easier to distinguish from native plants during some parts of the year. For example, Andrew and Ustin (2008) identified perennial pepperweed (*Lepidium latifolium*) during its flowering period, when it was spectrally most distinct from the surrounding marsh due to its unique white flowers. Temporally rich imagery can be used to identify the ideal time period for differentiation along with high spectral resolution to distinguish phenological differences. Third, the target IAS has a unique chemistry or biophysiology. For example, Khanna et al. (2011) differentiated water hyacinth from other co-occurring floating aquatic macrophytes using differences in canopy water content, since water hyacinth is a succulent with a higher plant-water content than co-occurring species water primrose (*Ludwigia peploides*) and water pennywort (*Hydrocotyle ranunculoides*). This requires a spectrally rich data set that is capable of quantifying canopy biochemistry. These three requirements are well matched with the three domains of RS data: spatial, temporal, and spectral.

Invasion detection often involves species mapping, which requires much more data than functional-type or general biodiversity mapping. Often hyperspectral imagery uses phenology to time the image capture and additional ancillary data such as altitude are necessary. As mentioned, sensors collect information in three primary domains: spectral, spatial, and temporal (an additional fourth domain, radiometric resolution, is critical for aquatic and marine applications – see Sect. 12.2.3 for more details). As a rule of thumb, hyperspectral imagery is rich in data in the spectral domain, aerial imagery from piloted and unpiloted aircraft in the spatial domain, and satellite imagery in the time domain. Each of these platforms and sensor types has trade-offs between the three domains and is typically only strong in one. Selecting the best platform/sensor and fusing the collected imagery with appropriate supplementary data results in the best classification maps. Each species and habitat presents unique challenges for identifying and mapping IAS using RS, which we elaborate upon further in the chapter. Regardless of habitat, the general process of detecting and mapping IAS remains the same and consists of the following steps (see also outlined Fig. 12.2):

1. *Identify the target species and/or area.* What IAS is affecting biodiversity, ecosystem services, or other economic functions in your area (e.g., transportation)? What do you know about your target IAS (e.g., spectral characteristics, phenology, ecosystem function, habitat requirements)? Do you know, or can you hypothesize, the IAS extent and community composition of other species in the area?

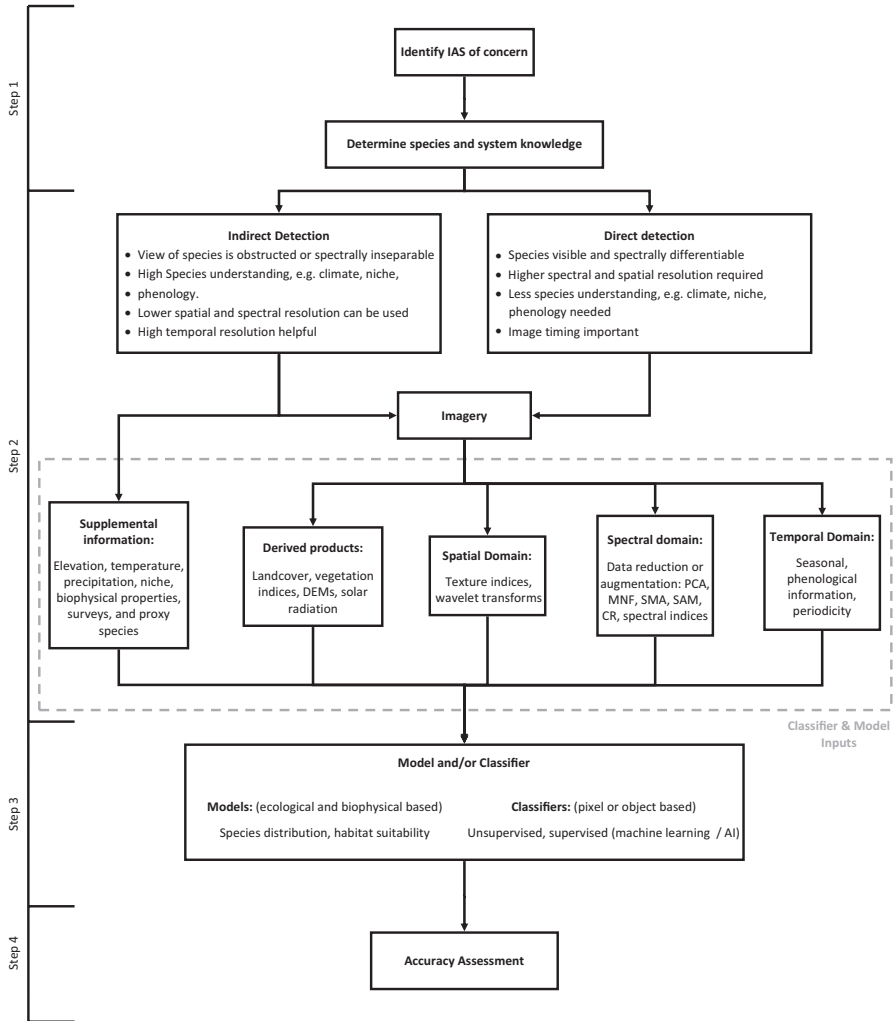


Fig. 12.2 General workflow for detecting IAS using RS. DEM, digital elevation models; PCA, principal component analysis; MNF, minimum noise fraction; SMA, spectral mixture analysis; SAM, spectral angle mapping; CR, continuum removal

2. *Determine the appropriate platform/sensor and identify/collect supplementary data based on species and habitat knowledge.* Target species can be detected using direct or indirect methods. Direct detection uses spectral data and derived products from imagery. Indirect detection utilizes the ecological relationships between species and their environment to predict distribution.

Each species and habitat discussed in this chapter has specific characteristics that can be exploited to detect IAS. Exploitable differences can exist in the temporal, spatial, or spectral domains. The temporal domain consists of data collection timing and revisit timing. For example, if an IAS flowers at an earlier or later

time than its surroundings, this information can be used to time image acquisition for when the target species appears most spectrally different. The spatial domain consists of pixel size and overall geographic coverage, and the spectral domain consists of the number of wavelengths, the position and bandwidth of wavelengths measured, and the spectral range of the sensor at which radiance can be measured reliably. Sensors typically have trade-offs among these domains based upon sensor design, size limitations, and data volume limitations. For example, in the spatial domain, there is a trade-off between overall coverage area or swath width and pixel size; both can be forced to increase, but at the expense of sensor size, which limits the platform it can be mounted on. There are also trade-offs between domains, mostly related to platforms. Most satellite platforms have larger pixel sizes than other platforms (20–100 s of meters) but have quick revisit time (days to weeks) and greater geographic coverage. Airborne platforms have a longer revisit time due to costs and logistics and smaller spatial coverage but offer smaller pixel size (centimeters to meters) and often support hyperspectral sensors. Unmanned aircraft systems (UAS) offer quick revisit time, on-demand deployment, and small pixel size but have very limited spatial coverage and limited spectral resolution due to size restrictions.

When direct detection is not possible due to canopy cover or other factors, indirect methods can be used to predict species locations. Species knowledge regarding habitat constraints or coexisting species can be used to govern a model using other data products. These data include things like digital elevation models (DEMs), climate layers, soil moisture, and any factor restricting species location. In some situations, these data can also be combined with direct detection methods to improve results.

3. *Enhance data and model/classify.* A model or classifier can be thought of as a set of rules or a mathematical function that uses pixel data to assign or predict class membership. This can either be supervised, where training data (pixels or spectra that have been identified previously) are used to define classes, or unsupervised, where classes are formed based upon pixel spectral/statistical similarity. Usually, atmospherically corrected surface reflectance data are provided to the classifier. Often, image enhancement is conducted to increase the information content of the input data. In addition to reflectance data, enhanced products can also be supplied to the classifier. Methods to enhance spectral data include spectral indices, principal component analysis (PCA), and minimum noise fraction (MNF). Spectral indices are combinations of spectral reflectance from two or more wavelengths that highlight a given reflectance or absorption feature and often indicate relative abundance of features of interest; for example, the Normalized Difference Vegetation Index (NDVI) is a normalized difference ratio of red and near-infrared (NIR) bands commonly used as an indicator of vegetation vigor.

With hyperspectral data, many narrowband indices are available that provide additional data about plant traits, including light use efficiency from the photochemical reflectance index (PRI; Gamon et al. 1997), canopy nitrogen from the normalized difference nitrogen index (NDNI; Serrano et al. 2002), canopy water content from the normalized difference water index (NDWI; Gao 1995), and a large number of leaf pigment indices [see Sims and Gamon (2002) for an

overview]. Continuum removal is another technique used to target absorption features. For each pixel reflectance, a convex hull is fit over the top of the spectrum, absorption features are normalized to that hull, and the depth of a specific absorption feature (e.g., leaf water content) can be quantified. PCA is a linear transformation method that maximizes the variance of the data. When applied to a hyperspectral image, it produces a series of components that correspond to linear combinations of the original bands aligned to represent the variation within the original data set, with the first component being the plane responsible for the most variation. This allows for determining the most significant characteristics within an image that relate to classes. Minimum noise fraction transformation (MNF) rescales the noise in the data (a process called noise whitening), enabling the analyst to eliminate bands containing too much sensor noise and leaving only coherent image data.

Commonly used classification techniques include random forest, a supervised machine learning algorithm that constructs many decision trees and utilizes their outputs to get an accurate class prediction based upon training data, and maximum likelihood estimation (MLE), a supervised classification method in which parameter values of a statistical model are determined that maximize the chance that the process described by the model was actually observed. All of these data enhancement and classification methods can be performed using open-source software, such as R (<https://www.r-project.org/>) and Python (<https://www.python.org/>), where many packages are available to use, or in commercial software, such as ENVI (<https://www.harrisgeospatial.com/>).

4. *Assess accuracy.* One of the most important considerations is accuracy assessment following mapping. Depending on the objectives of the study, some types of error may be acceptable, while some may not. Typical accuracy metrics for image classification include overall accuracy, user's accuracy, producer's accuracy, and Kappa coefficient. Overall accuracy is the probability that an image classifier will correctly classify a pixel. This metric does not account for the number of validation pixels per class and may be misleading if a similar number is not used for each class. User's accuracy and producer's accuracy may be better metrics for assessing the classification. User's accuracy (error of commission) is the fraction of correctly classified pixels with regard to all pixels classified. Producer's accuracy (errors of omission) is the fraction of correctly classified pixels with regard to all ground reference validation pixels. In some situations, such as automated weed management in agriculture, overall accuracy and producer's accuracy may not be as much of a concern as user's accuracy because identifying small amounts of weeds (IAS) as crops may be okay, but spraying crops misidentified as IAS could be more damaging to crop yields than the IAS themselves. An example where maximizing producer's accuracy may be more important would be in mapping IAS to understand species spread and the invasion process; any omitted species data as changes are monitored over time could affect process understanding and spread predictions. The last metric, the Kappa coefficient, can be useful for comparing multiple classification methods within the same data set. The Kappa coefficient is a measure of how closely the resulting

overall accuracy of a classifier compares with expected accuracy, a random classification of pixels from the data set. One final consideration for accuracy assessment is the importance of having independent validation data that were not used in the mapping procedure. If accuracy is assessed with training data, it only measures how good the classifier is for those specific data that it was trained on, but the classifier may not be as accurate with other non-training pixels within the image.

12.2 Invasive Plants in Natural and Agroecosystems

Each ecosystem and IAS combination presents unique challenges for identification and mapping using RS. This is due to different landscape configurations, community composition, canopy structures, climates, habitat characteristics, and plant phenology. Each of these characteristics can be used to inform the optimal instrumentation for IAS detection and mapping. For this reason, we have separated IAS detection methods by biome and then split into more specific ecosystems and case studies.

12.2.1 Forests

Around one-third of Earth's land surface is covered by forests. Forests are critical ecosystems, holding a very large proportion of global biodiversity. They are responsible for a large fraction of the global carbon storage and fluxes, strongly influence local and global water cycle processes, and provide fundamental goods and services to humanity (Foley et al. 2007). Globally, there are 26 types of forests, from taiga to tropical, all characterized by the unique ecological adaptations of trees to local climate, geology, and ecological conditions.

Forests invasions come in two types: (i) tree invasions (13 trees are in the top 100 world's most invasive alien species, Lowe et al. 2000); and (ii) when other plants, such as vines and shrubs, or animals invade (Resasco et al. 2007; Cheng et al. 2007; Santos and Whitham 2010). Detection of invasion by tree species requires the direct detection of tree canopies (e.g., Asner et al. 2008a, b). Invasion of forests by other plants or animals can be detected directly, for example, when the IAS covers the canopy (Cheng et al. 2007), or indirectly, by measuring canopy leaf-off (Resasco et al. 2007; Wilfong et al. 2009), or through detection of pest impacts (Näsi et al. 2015; Ortiz et al. 2013).

Several studies have used optical RS data to directly detect invasion by tree species. One of the earliest approaches performed texture analysis on simulated satellite panchromatic imagery from historical 2 m aerial photography to map the invasive acacia (*Acacia mearnsii*) in South Africa (Hudak and Wessman 1998). Ramsey III et al. (2002) used 0.5 and 1.0 m color-infrared aerial photographs to map Chinese tallow (*Sapium sebiferum*) in Louisiana and Texas. They used a k-means

classifier to discriminate IAS with relative success, attributed to the differences in senescence colors between the IAS and the native vegetation. A subsequent study scaled this approach to satellites, using a combination of Hyperion, Landsat 5, and aerial photos to define characteristic spectral signatures from 400 to 950 nm for Chinese tallow (Ramsey III et al. 2005). Pearlstine et al. (2005) also used aerial photos with larger spatial resolution (37×25 m) to map Brazilian pepper tree (*Schinus terebinthifolius*) using texture analysis on red, green, and NIR bands to identify the IAS relatively well.

Multispectral satellite data have been used to map tree IAS with varying levels of success. Fuller (2005) performed a supervised classification of IKONOS (2 m) and Landsat ETM+ (30 m) data to detect broad-leafed paperbark (*Melaleuca quinque-nervia*) in Florida; the timing of imagery was chosen to enhance IAS separability. Cuneo et al. (2009) also used Landsat Enhanced Thematic Mapper (ETM) data to map African olive (*Olea europaea cuspidata*) in Australia based on spectral dissimilarity with the native *Eucalyptus* spp. with an accuracy of 85% and very low confusion between the species. More recently, decadal-scale time series afforded by sustained land imaging have enabled increased accuracy in cases where phenological cycles can distinguish IAS. Diao and Wang (2016) used a long time series to use the phenological changes in tamarisk for high-accuracy classification. Hoyos et al. (2010) mapped glossy privet (*Ligustrum lucidum*) in Argentina using a time series of Landsat TM data and machine learning (support vector machines, SVM), achieving classification accuracies of 89%.

Several studies used imaging spectroscopy to map tree IAS (He et al. 2011; Bradley 2014), e.g., tamarisk (Hamada et al. 2007; Carter et al. 2009), black cherry (*Prunus serotina*), black locust (*Robinia pseudoacacia*) and northern red oak (*Quercus rubra*) (Boschetti et al. 2007), Brazilian pepper (Lass and Prather 2004), and fire tree (*Myrica faya*) (Asner et al. 2008a, b). The studies determined characteristic IAS spectral profiles (sensu Ramsey III et al. 2005), compared spectral profiles across species using techniques such as SAM (e.g., Lass and Prather 2004), and correlated them with ground measurements (e.g., Asner et al. 2008a, b).

Lidar in combination with imaging spectroscopy has been found useful for assessments of tree IAS (Huang and Asner 2009). For example, Asner et al. (2008a, b) combined imaging spectroscopy and lidar to detect fire tree in Hawaii and measure impacts on forest canopy biochemistry (Fig. 12.3). Hantson et al. (2012) mapped black cherry and beach rose (*Rosa rugosa*) in the Netherlands, finding that the additional height information from lidar improved classification accuracy by 12% over imaging spectroscopy data alone.

Direct detection of IAS on the tree canopy has also been studied. For example, Cheng et al. (2007) used imaging spectroscopy to detect kudzu (*Pueraria montana*) in a pine forest in Western Georgia, United States. They used an MNF transform and SAM to differentiate the spectral profile of the IAS from the native forest. Wu et al. (2006) mapped the invasive climbing fern (*Lygodium microphyllum*) in the Florida Everglades with a supervised classification of IKONOS imagery to show how it established in different parts of the forest. Although successful, their results underestimated fern extent in the understory.

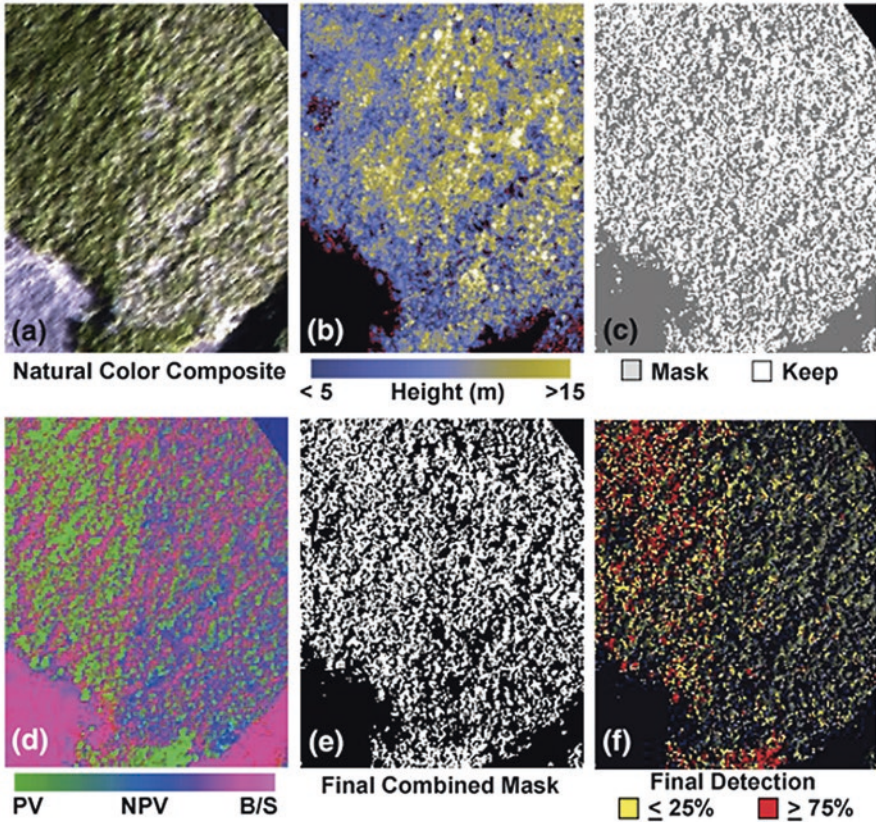


Fig. 12.3 Example output of each automated analysis step in the hyperspectral-lidar data fusion and invasive species detection process from Asner et al. (2008a, b). This 53 ha example of the study site in Hawaii shows (a) basic reflectance imagery that demonstrates the prescreening of the spectrometer image data by (b) minimum vegetation height modeling from lidar data (ground, black; shorter canopies, red/dark blue; taller canopies, yellow/white); (c) shadow masking based on 3-D structure of the canopies with respect to solar angle and sensor geometry (shadow, gray; sunlit, white); (d) live/dead fractional cover masking from AutoMCU (a spectral mixture analysis) modeling (PV, green; NPV, blue; bare/shade, pink); and (e) the final detection of an invasive tree based on spectral endmember bundles and AutoMCU-S algorithm (invader, yellow/red; native, green)

Indeed, invasion of the forest understory is relatively understudied. Dense canopies mask understory contribution to the RS signal. To address this, researchers have turned to leveraging forest phenology to directly detect the understory when it is most visible. Resasco et al. (2007) mapped the historical spread of Amur honeysuckle (*Lonicera maackii*) during leaf-off conditions of the native forest using the Soil Adjusted Atmospheric Resistant Vegetation Index calculated from Landsat TM and ETM+ from 1999 to 2006. Wilfong et al. (2009) found that using a difference image measuring the difference between leaf-on and leaf-off conditions better pre-

dicted Amur honeysuckle cover than a single image. Evangelista et al. (2009) used a species distribution model to predict tamarisk (*Tamarisk ramosissima*) distribution over time based on vegetation indices derived from Landsat ETM+ data, with a 90% classification accuracy. Kimothi et al. (2010) used Indian RS satellite data to map another understory IAS, the West Indian lantana (*Lantana camara*), using texture analysis of images from September, February, and April. The dense leaf canopy meant separation of IAS was not possible in September, but classification accuracies were >90% in the other images after leaf fall. Barbosa et al. (2016) mapped subcanopy strawberry guava (*Psidium cattleianum*) outbreak with imaging spectroscopy and lidar and tested the accuracy of a machine learner, biased-SVM (BSVM), and mixture-tuned matched filtering (MTMF; a partial unmixing classification algorithm similar in principle to MNF) across canopy layers. While both methods allowed the estimation of the fraction of canopy layers that were invaded, the BSVM used information across the entire spectrum, while the MTMF did not, which may limit the applicability of MTMF when spectra of IAS are similar to “background” native species.

Indirect methods are another alternative to study understory IAS. Joshi et al. (2006) mapped Siam weed (*Chromolaena odorata*) in the understory using Landsat ETM+ and an artificial neural network to predict forest density and canopy light penetration and then subsequently predict Siam weed seed production. They found that 93% of the IAS seed production was predicted by the light intensity reaching the understory and concluded that this method worked relatively well to detect the IAS, despite the spatial resolution limiting detection to well-established IAS patches.

In summary, the most common method to detect tree IAS and map their distribution are to use their characteristic spectral signatures and dissimilarity with that of the native vegetation (Lass and Prather 2004). Tree IAS likely affect both the forest's spatial structure as reflected in texture metrics (Pearlstine et al. 2005) and its 3-D structure, as shown with lidar (Asner et al. 2008a, b). To maximize the ability to detect invasive tree species, the use of the full visible (VIS) to shortwave infrared (SWIR) spectrum with imaging spectroscopy has shown clear advantages (Martin, Chap. 5), for example, in detecting the fire tree (Asner et al. 2008a, b) and for detecting bamboo (*Dendrocalamus* sp.) and slash pine (*Pinus elliottii*; Amaral et al. 2015). Alternatively, other studies selected specific bands that maximized discrimination and eliminated potential noise from nondiscriminating parts of the spectrum (Boschetti et al. 2007). While the advantages of imaging spectroscopy are obvious, data are not yet readily available to detect and map many tree IAS, especially in early stage invasion stages, although the upcoming launch of several hyperspectral satellite sensors will soon change this. Many tree IAS have different phenology than the native forest, either staying green longer, greening earlier, or flowering or budding later (Landmann et al. 2015); or they may be evergreen in a deciduous forest (Diao and Wang 2016). Timing imagery acquisition to maximize phenological differences has resulted in good classification accuracy (Ramsey III et al. 2002). Finally, using pixel sizes that match a tree canopy allows the detection of single

invading trees (Bradley 2014). However, this can be very time-consuming, costly, and perhaps less systematic and viable across large areas or for early detection.

There are several analysis considerations for mapping tree IAS. A first, and perhaps most important, aspect is that tree IAS detection is prone to higher classification error (Bradley 2014) than other classifications, given the similarity in the spectral characteristics of trees to each other relative to other plant functional types. Spectral similarity between invasive and native trees may influence accuracy (Lass and Prather 2004), so ensemble classifications are recommended as well as other approaches that maximize spectral differences such as taking into account phenology. The examples cited above illustrate the value of a good field sampling design (Ramsey III et al. 2002) that covers the diversity of canopy structures (Hudak and Wessman 1998) and community compositions within the area of interest, since heterogeneity affects overall classification accuracy. In all of the studies discussed here, we observed a trade-off between omission and commission errors, where classification accuracy seems to be positively correlated with commission errors. Thus, we recommend that several accuracy metrics should be reported rather than just overall accuracy to give a better understanding of which species contribute to commission errors and which areas are more uncertain in IAS distribution maps.

12.2.2 *Rangelands and Grasslands*

Grasslands cover approximately one-third of the Earth's surface (Latham et al. 2014), account for at least 30% of primary production by terrestrial vegetation (Grace et al. 2006), and, after forests, are the largest terrestrial carbon sinks (Anderson 1991; Derner and Schuman 2007; Grace et al. 2006). There are two main classes of grasslands, tropical/subtropical (also known as savanna) and temperate, which can further be described by three different subclasses: human generated, highly managed natural, and rangelands (Ali et al. 2016). Regardless of classification, these regions serve as a major source of animal feed and are heavily influenced by changes in climate and fire dynamics (D'Antonio and Vitousek 1992; Brooks et al. 2004). Contrary to popular belief, grasslands and rangelands harbor large amounts of biodiversity (Murphy et al. 2016); however, they are under threat as IAS continue to invade. This threatens biodiversity not only through direct losses by IAS replacing native grasses but also through indirect impacts to ecosystems by changing fire regimes (D'Antonio and Vitousek 1992; Balch et al. 2013), supporting wind erosion (Weisberg et al. 2017), and serving as a facilitator for plant viruses (Ingwell and Bosque-Pérez 2015).

IAS in grasslands may be monitored directly or indirectly because not all species or all grassland ecosystems are good candidates for RS measurements. IAS in grasslands can be difficult to monitor. They are often indistinguishable from native plants due to spectral similarities or the nature in which they grow—in small patches, mixed with native vegetation (Shafii et al. 2004). Often indirect methods are most appropriate because they do not rely solely on discrimination between similar

vegetation functional types. Indirect methods include multisource data for inferring IAS distributions and coupled RS observations and modeling. For example, the National Land Cover Database (NLCD), which is derived from Landsat data, has been used in combination with EROS Moderate Resolution Imaging Spectroradiometer (eMODIS) vegetation products (Jenkerson et al. 2010) to create a cheatgrass index based on phenology (Fig. 12.4; Boyte et al. 2015). Climate variable models such as Daymet (Thornton et al. 2018) that use DEMs created from Shuttle Radar Topography Mission (SRTM) data have been used in combination with eMODIS vegetation products to monitor the spread of cheatgrass (Downs et al. 2016).

Phenological differences are helpful for distinguishing native from non-native grasses. Given their frequent temporal resolution and global coverage, satellite optical sensors, such as Landsat TM/ETM+/OLI, SPOT, Sentinel-2, or, in some cases, Moderate Resolution Imaging Spectroradiometer (MODIS), have been used in several studies to map invaded grasslands. Cheatgrass, one of the top invaders in North America, greens up in early spring and senesces before native grasses, making it a suitable target species for RS approaches that leverage phenology differences (Fig. 12.4). Various studies across the United States have paired field data with multi-seasonal imagery selected during the green up (April–May) and senescent period to successfully map cheatgrass spread (Peterson 2005; Singh and Glenn 2009;

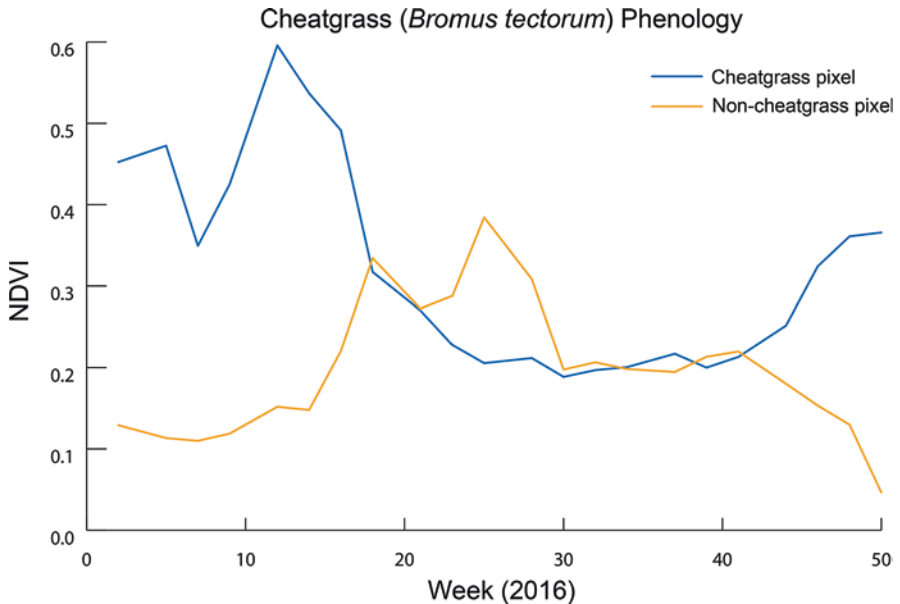


Fig. 12.4 Cheatgrass phenological differences from native sagebrush (*Artemisia* spp.) shown using eMODIS NDVI. Note that sagebrush (non-cheatgrass) greens up later in the year, allowing for development of the cheatgrass index (Boyte et al. 2015; Boyte and Wylie 2017)

West et al. 2017) and die-off (Boyte et al. 2015; Weisberg et al. 2017). Rather than just using images selected during green up and senescence periods, extracting phenology metrics from vegetation indices to refine cheatgrass classifications has also been successful (Bradley and Mustard 2008); however, in arid and semiarid environments, these indices can be highly influenced by rock and soil and should be used with caution (Singh and Glenn 2009). Huang and Geiger (2008) showed that a multi-date imaging approach can be successful even when natural phenologies of natives and nonnatives are similar. For example, native grasses and Lehmann lovegrass (*Eragrostis lehmanniana*) responded differently to unusual amounts of cool season precipitation, which allowed new tissues in invasive species to grow, making the two grasses distinguishable with multi-date imaging (Huang and Geiger 2008).

Imaging spectroscopy to map grassland IAS also often depends on differences in phenology, but the higher spectral resolution and typically higher spatial resolution afforded by airborne platforms often allow for more detailed and early detection maps. Image acquisition timing is important for species that exhibit differences in coloration throughout the year, such as flowering species or deciduous shrubs. In the case of leafy spurge (*Euphorbia esula*), hyperspectral instruments are better equipped to detect changes in flowering and thus have a higher success rate when compared to multispectral instruments (Mitchell and Glenn 2009). Leafy spurge has characteristic yellow flowers that bloom in early summer, and tamarisk leaves turn from yellow-orange to orange-brown in autumn before leaf drop. This distinct pigmentation enables remote detection using both imaging spectroscopy (Williams and Hunt Jr 2002; Glenn et al. 2005) and multispectral data (Anderson et al. 1993; Everitt et al. 1995; Evangelista et al. 2009). The blue-green color of new stems and the red-brown color of older stems help detection of spotted knapweed (*Centaurea maculosa*) from imaging spectroscopy (Lass et al. 2002; Lawrence et al. 2006). For early detection of goldenrod (*Solidago altissima*), an invasive moist tall grass in Japan, hyperspectral images acquired during early spring before full development of the grass canopy make it easier to map the exposed understory (Ishii and Washitani 2013).

Differences in canopy architecture or plant morphological traits, such as plant height and pubescence, can also be exploited when plants share similar phenologies or imagery is unavailable when growth cycles show key differences. Broom snake-weed (*Gutierrezia sarothrae*), for example, has an erect leaf canopy structure that results in a dark image response (Everitt et al. 1987; Yang and Everitt 2010). Spotted knapweed tends to inhibit the growth of other vegetation; the resulting increase in visible bare soil can help identify places where spotted knapweed grows (Lass et al. 2002; Lawrence et al. 2006).

In summary, multispectral sensors that provide free and open access to global imagery are used regularly for IAS detection in grasslands because their predefined temporal resolution offers recurring overpasses and at the very least provides seasonal imagery. This supports time series analyses and multi-date classification techniques. Looking to the future, changes in grassland species composition are anticipated to have the largest impact on Africa because it is home to the largest savannas, which cover roughly 50% of the continent (Campbell 1996; Grace et al.

2006). In addition, savannas in South American and Central Asia and temperate grasslands in the Western United States will also be heavily impacted. Thus, free, open-access, global mapping satellite RS data sets are especially important for grassland IAS detection and monitoring. These sensors lack the fine spatial resolution and full spectrum afforded by airborne imaging spectroscopy, which may be necessary to separate native and non-native species of the same functional type. However, multispectral imagery is often used for viewing widespread and abundant invasives, which is key for monitoring overall ecosystem invasion onset and die-off, but offers little help in terms of real-time or early IAS detection. In both cases, the minimum percent cover required for mapping can vary across similar ecosystems (Bradley 2014) and depends on sensor resolution and on how distinguishable the invader is from the background. Even when a non-native grass is spectrally distinguishable, an acceptable detection rate is not always possible when patch sizes are small relative to pixel resolution (Mladinich et al. 2006). Therefore, to ensure successful mapping, IAS targets must differ from the native community spectrally, phenologically, texture/morphologically, or architecturally (Bradley 2014). Analysis considerations must include a careful evaluation of the relationship between vegetation characteristics and sensor resolutions, particularly in the spatial, spectral, and temporal domains.

12.2.3 *Aquatic Ecosystems*

Although they cover a small portion of the Earth's surface, aquatic ecosystems are disproportionately important to global diversity. They are among the most diverse and productive ecosystems on Earth and provide vital ecosystem services (Tabacchi et al. 1998; Barbier et al. 2011). Aquatic ecosystems encompass multiple gradients, such as water intermittency, microtopography, and salinity, leading to complex environmental heterogeneity (Junk et al. 1989; Mitsch and Gosselink 2007). This mosaic of diverse environmental conditions supports high biodiversity through multiple niches (Tockner et al. 2000; Ward et al. 2002).

Biodiversity losses in coastal and freshwater aquatic ecosystems are among the highest in the world (Dudgeon et al. 2015; Waycott et al. 2009; Vörösmarty et al. 2010). At least 30%–50% of the world's wetlands have been lost (Finlayson 2012; Hu et al. 2017), and up to 35% of the extent of critical habitats like seagrasses and mangroves have been destroyed just in the twentieth century (UNESCO 2018). These ecosystems are among the most vulnerable to invasion because they are highly connected, are used extensively by humans, and often are geographically close to invasion foci such as ports or urban areas (Gherardi 2007; Williams and Grosholz 2008).

Plants in aquatic ecosystems can be broadly classified into five functional types or sets of species that occupy distinct spatial niches along the gradient from water to land and often have similar characteristics. The five functional types considered

here are from land to water: riparian forests with shrubs and trees, emergent reeds and sedges, floating macrophytes, submerged macrophytes and macroalgae, and phytoplankton. Differentiating among these functional types with RS is achievable, but species-level detection within each community is more difficult due to similar survival strategies. Each functional type has its own challenges regarding species detection.

Many studies have successfully mapped IAS in aquatic environments using direct detection. Depending on the objectives of the study and the functional type being examined, spectral, spatial, and temporal requirements vary. In simple systems, high spatial resolution aerial photos can often be used to map species functional types as well as single species by taking advantage of unique attributes or phenology (Marshall and Lee 1994; Everitt et al. 1999, 2003). Mapping multiple species within the same functional types has been less successful using aerial photos. In these situations, more spectral information is needed to differentiate at the species level due to varying community complexity and species attributes (e.g., Khanna et al. 2011). Multispectral data have also been used with varying levels of success to map IAS in simple systems such as lakes invaded by just one species (essentially a two-class system; Venugopal 2002) or lakes with floating and some submerged vegetation (a three-class system; Everitt et al. 2003; Verma et al. 2003; Albright et al. 2004). Many classification methods have been used within aquatic ecosystems with varying degrees of success, including unsupervised classifiers, such as k-means and ISODATA (Ackleson and Klemas 1987; Dogan et al. 2009) and simple supervised classifiers, such as maximum likelihood and minimum distance (Malthus and George 1997; Vis et al. 2003; Nelson et al. 2006; Jollineau and Howarth 2008; Phinn et al. 2008; Yuan and Zhang 2008; Dogan et al. 2009), as well as more advanced machine learning methods (Malthus and George 1997; Nelson et al. 2006; Hestir et al. 2008, 2012; Everitt et al. 2011; Santos et al. 2012, 2016). While some studies have been successful and have even been operationalized into routine monitoring for invasive species management and reporting (sensu Santos et al. 2009; Santos et al. 2016), in many studies it is difficult to judge classification efficacy because accuracy assessment is missing or unusual, often not having independent validation data. Overall, machine learning algorithms seemed to have performed best. Within functional types, some specific strategies seem to work best as well. We highlight these below.

12.2.3.1 Riparian

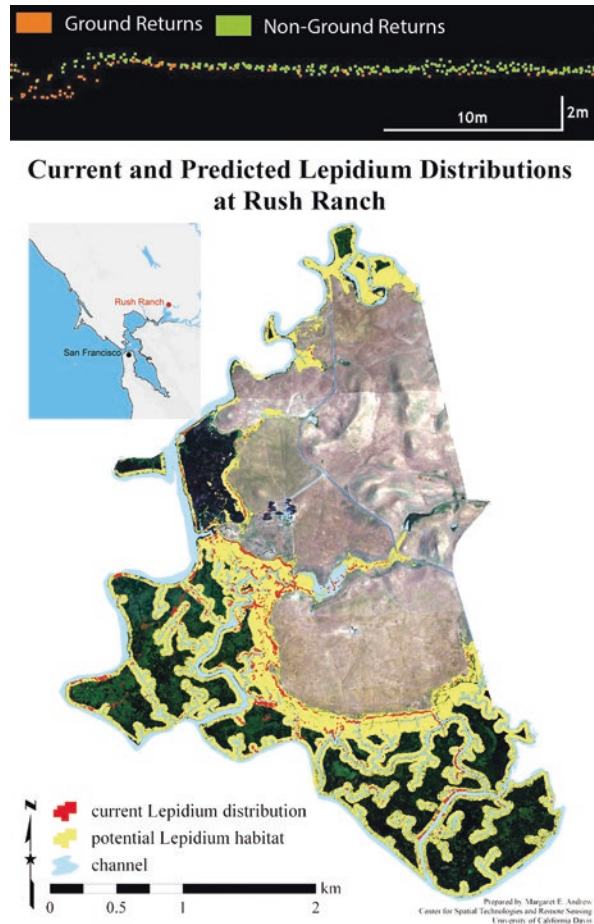
Riparian plants are often more difficult to differentiate at the species level than emergent and floating plants due to higher number of species and life forms, and a complex canopy structure, similar to forest IAS detection. Riparian IAS sometimes grow in monocultures, which may be easier to detect (e.g., giant reed, *Arundo donax*). Other IAS can grow embedded in the native community similar to grasslands, making them harder to map using RS (e.g., yellow star-thistle, *Centaurea solstitialis*).

From an RS perspective, the layered canopy, many species, and mixed pixels make it hard to map target IAS within this complex community mosaic.

Community complexity can often be overcome by taking advantage of differences in phenology. Acquiring imagery during flowering or senescence when the target IAS is most distinct from its surrounding vegetation may allow for detection at the species level. For example, Landsat ETM+ and QuickBird have been used to take advantage of correct timing and fine spatial resolution, respectively, to distinguish riparian IAS (Laba et al. 2008; West et al. 2017). Frequently, increasing spectral data further has been necessary to detect riparian IAS. (Ustin et al. 2002; Laba et al. 2005; Hamada et al. 2007; Andrew and Ustin 2008).

Another concept used to map riparian plants is adding contextual information such as distance from channel and elevation (Fig. 12.5; Andrew and Ustin 2009). Contextual information can also help in improving accuracy of detection across various techniques (Maheu-Giroux and de Blois 2005; Andrew and Ustin 2008) or

Fig. 12.5 A sample vertical cross-section of the lidar returns on a transect perpendicular to a given channel shows the relationships among ground cover, elevation, and distance to a channel at Rush Ranch, California, USA (top). Current and predicted distribution (3 m window topography model) of perennial pepperweed at Rush Ranch, California, USA, overlain on a true color mosaic of airborne hyperspectral imagery (HyMap). Potential distribution was mapped as the majority rule of 25 individual classification tree models (bottom). (Derived from Andrew and Ustin (2009))



in building species occupancy models based upon species ecological knowledge to predict future invasions or direction of spread (Andrew and Ustin 2009; Rocchini et al. 2015).

12.2.3.2 Emergent

Within the emergent functional type, the canopy is relatively uniform, composed generally of only grasses, sedges, and reeds. These species are often mixed, and patch sizes remain small even among species tending to grow as monocultures. The canopy structure is typically erectophilic, and spectral mixing with water is common, even with fine spatial scale imagery. In addition to spectral information and temporal information, the texture of invasive and native species patches can be leveraged in mapping IAS and may be used to improve success. Samiappan et al. (2017) used four methods to calculate texture indices as inputs into a SVM algorithm to map common reed (*Phragmites australis*). They took advantage of the 5 m spatial resolution afforded by airborne (in this case UAS) imagery, though they cautioned such an approach is unlikely to work if patches of IAS are smaller than a few pixels or more mixed. However, texture has been shown to be advantageous even with moderate spatial resolution imagery. For example, Arzandeh and Wang (2003) successfully differentiated common reed and cattail (*Typha angustifolia*) using Landsat TM by adding texture indices to increase pixel spectral information content. For these reasons, hyperspectral aerial surveys have offered the best data source for classifications for emergent communities. Using sensors such as CASI, AVIRIS, and HyMap, many studies have mapped the emergent community, differentiating species within submerged and floating functional types (Hestir et al. 2008; Jollineau and Howarth 2008; Hunter et al. 2010; Khanna et al. 2011; Hestir et al. 2012; Zhao et al. 2012). Occasionally, both spectrally rich and temporally strategic data have been used together to map IAS (Laba et al. 2005; Hamada et al. 2007; Pu et al. 2008).

12.2.3.3 Floating Macrophytes

Floating macrophytes have a simple canopy structure with vegetation growing close to the water surface. They can spread over large areas and often grow as monocultures, so mapping them using RS has been relatively easy, except when two or more floating species co-occur in a single ecosystem (Khanna et al. 2011; Cavalli et al. 2009). Floating macrophyte mats often appear very similar spectrally, for example, water hyacinth, water primrose, and pennywort (*Centella asiatica*) (Khanna et al. 2011). Cavalli et al. (2009) separated three floating species with Landsat ETM+ data using spectral linear mixture modeling trained by high-quality spectral libraries developed from field spectroscopy. However, without detailed spectral libraries for a location, hyperspectral data are needed to differentiate between similar, bright green uniform mats of floating species (Yang 2007; Khanna et al. 2011).

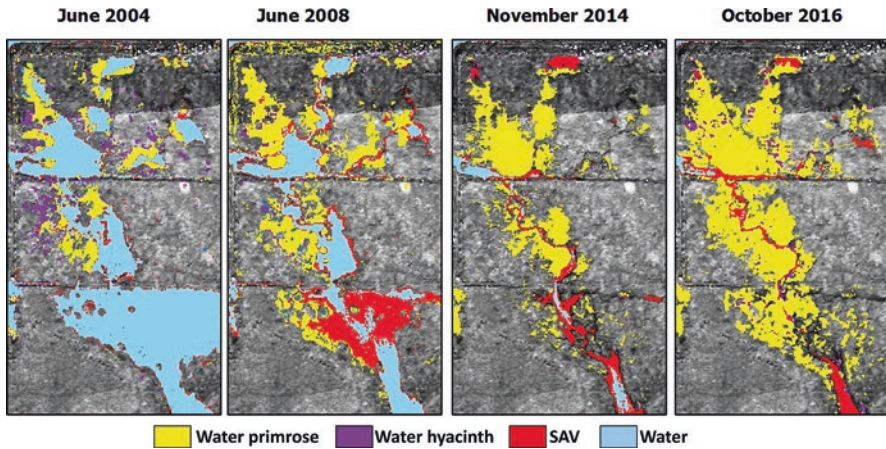


Fig. 12.6 Water primrose expansion into open water and submerged vegetation habitat (June 2008 and November 2014) and finally into emergent marsh habitat (October 2016). (Reproduced from Khanna et al. 2018)

Using hyperspectral data from HyMap and AVIRIS, Khanna et al. (2018) monitored how water primrose spread over a 12-year period (Fig. 12.6) and showed how it fundamentally changed biophysical and ecological characteristics of the ecosystem, including successional pathways.

12.2.3.4 Submerged Macrophytes

Mapping submerged macrophytes and macroalgae presents additional challenges due to the presence of the water column. Detection of these plants is complicated by the combined effects of inherent optical properties (IOPs) of the water column, which are influenced by the diffuse attenuation of the water column itself and the absorbing and scattering properties of its dissolved and suspended matter, and the apparent optical properties (AOPs), which are controlled by weather, sun, and sensor view angles (which can lead to sun glint or insufficient signal returns) as well as the influence of the air-water interface (Mertes et al. 1993; Bostater Jr. et al. 2004; Morel and Bélanger 2006; Hestir et al. 2008). IOPs are difficult to account for because water quality and depth can vary spatially and temporally with runoff, geomorphological gradients, meteorological conditions, flow conditions, land use practices, tidal stage, and phytoplankton phenology and community changes (Vis et al. 2003; Nelson et al. 2006; Hestir et al. 2008). Radiative transfer approaches are useful for classifying submerged species. Typically, they use either use model inversion or look-up tables to solve the radiative transfer model in the water column to distinguish different optically active constituents (e.g., phytoplankton and other pigments, suspended non-algal particulates, colored dissolved organic matter) and differentiate bathymetry and bottom type (see Odermatt et al. 2012; Giardino et al. 2018 for

comprehensive reviews of the approach). These approaches are often preferred because, being physics-based, they are in principle generalizable and transferable across sensors and systems (Giardino et al. 2010, 2012; Malthus et al. 2012; Hestir et al. 2015). However, such approaches require detailed spectral information on specific water body IOPs, which are difficult to collect and not generally available (Matthews 2011; Lymburner et al. 2016). In these approaches, bottom type is typically mapped to just a few broad classes (e.g., sand/sediment, rock, submerged plants, coral), so species-level detections are not common in the literature (Dörnhöfer and Oppelt 2016). However, Santos et al. (2012) were able to show species-level discrimination of submerged macrophytes at the leaf level and could differentiate native from non-native submerged macrophytes at the canopy level from HyMap airborne imaging spectroscopy in a turbid estuary in California.

Often the dominant species is invasive, so even community-level maps can still reveal important processes about IAS spread and persistence and the effects of invasion on ecosystem function. Santos et al. (2016) successfully mapped submerged macrophyte spread and persistence over several years using the airborne imaging spectrometer HyMap, highlighting invasion pathways (Fig. 12.7) in the upper San Francisco estuary in California, USA. Hestir et al. (2008, 2012) mapped submerged aquatic vegetation using the same airborne imaging spectrometer and used those maps to show that increased vegetation cover significantly contributed to the increased water clarity of the system (Hestir et al. 2016).

To circumvent some of the confounding factors of the air-water interface and water column for mapping submerged macrophytes, hydroacoustics are often used for bed delineation and height and density quantification (Winfield et al. 2007). These require intensive boat surveys (which limit access), do not provide species-level discrimination, and can provide significantly different results for the same system due to lack of standardization in signal processing approaches (Radomski and Holbrook 2015). Recently it has been argued that RS imagery approaches are, despite several limitations, overall more efficacious than hydroacoustic surveys (McIntyre et al. 2018).

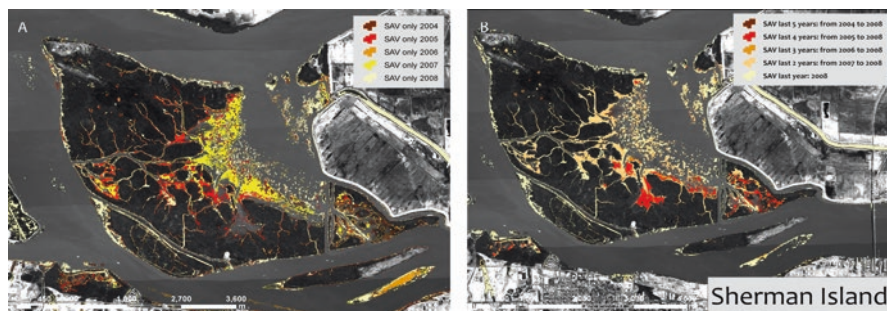


Fig. 12.7 (a) Map of submerged aquatic vegetation (SAV) spread near Sherman Island, CA, from 2004 to 2008. (b) Map of SAV persistence from 2004 to 2008 at Sherman Island, CA

12.2.3.5 Phytoplankton

Commercial shipping and the exchange of ballast water is one of the main pathways of IAS spread in marine and aquatic environments around the world. It is difficult to characterize phytoplankton species as native or non-native due to limited inventories, varying morphology and complex synonymy based on regional environmental differences, and the spontaneous “appearance” of new species (Olenina et al. 2010). Nonetheless, many phytoplankton species have been documented to have spread via ballast water (Subba Rao et al. 1994; Olenin et al. 2000), and species recorded in ships’ ballast water are increasing in abundance (Olenina et al. 2010). Rapid shifts in species composition and large harmful algal blooms in coastal and inland waters have cascading effects on community structure for waterfowl, marine mammals, fish, shellfish, and benthic communities and are a constant concern for biodiversity conservation and ecosystem managers (Anderson et al. 2002).

In the water column, different phytoplankton pigments have key spectral absorption features that can be resolved in order to make inferences about their functional type. Chlorophyll a, the key diagnostic pigment for many diatoms, absorbs strongly at 435–438 and 660 nm. Cyanobacteria, the common culprit of large-scale harmful “blue-green” algal blooms, show absorption features at 490–625 nm. Floating algae have spectral features in the 550–900 nm range. *Mesodinium rubrum*, the photosynthetic ciliate that causes red tides, contains the pigment phycoerythrin, which fluoresces in the yellow peak (565–570 nm; Dierssen et al. 2015).

With the exception of key diagnostic pigments that allow direct estimation of the concentration of certain species (e.g., coccolithophores, *Mesodinium*), RS of phytoplankton species is typically limited to detection of phytoplankton functional types or groups (based on taxonomic criteria or biogeochemical function) or phytoplankton size class (based on size range) (Bracher et al. 2017). Most detection algorithms rely on radiative transfer models that account for bio-optical properties (e.g., pigment composition, absorption, and backscattering), empirical relationships that relate chlorophyll a concentrations measured via satellite with in-situ measurements of diagnostic marker pigments determined from high-performance liquid chromatography (HPLC) or ecological models that predict phytoplankton functional type presence based on different abiotic and biotic parameters. Moisan et al. (2012) and Bracher et al. (2017) provide an overview on the state of the science for RS phytoplankton species detection. Sathyendranath et al. (2014) and Mouw et al. (2017) provide details on most of the current algorithms and procedures for phytoplankton functional type mapping from RS.

Mapping phytoplankton functional types in coastal and inland waters is still challenging, however. Current land missions lack the temporal resolution to make frequent, repeated observations at the scale of tidal, riverine, meteorological, and biotic processes (e.g., growth, grazing, senescence) that drive phytoplankton variability (Muller-Karger et al. 2018). Phytoplankton and water quality change on the scale of hours to days due to runoff, advection, and mixing. Kudela et al. (2015) used time series of field hyperspectral observations to show that phytoplankton blooms can be displaced by cyanobacteria in a few days. Hestir et al. (2015)

documented similar rapid changes in cyanobacteria from hyperspectral measurements. Chen et al. (2010) observed phytoplankton blooms that evolve over 2–3 days in Tampa Bay. After 13 years of observations in Long Island Sound, Dierssen et al. (2015) concluded that monthly measurements are insufficient to quantify episodic plankton blooms. While they documented a bloom of a ciliate that could only be detected with hyperspectral measurements, of yellow fluorescence, only one such image has ever been collected of this area and this was with the Hyperspectral Imager for the Coastal Ocean (HICO) that ceased operations in 2014.

Mapping submerged phytoplankton, macrophytes, and macroalgae is one of the most challenging aspects of IAS detection in aquatic systems. Well-calibrated hyperspectral data with good radiometric quality is crucial when mapping submerged phytoplankton, macrophytes, and macroalgae to the species level. Due to the low reflectance, noise can severely affect data. Because of signal attenuation within the water column, typically less than 10% of the signal measured at the top of the atmosphere comes from the water column and the submerged community. The reduction in signal as water depth increases above submerged species can be seen in Fig. 12.8. Thus, atmospheric correction, sensor performance, accuracy, and radiometric quality are especially important for the water column and submerged aquatic macrophytes (Muller-Karger et al. 2018). Space-based sensors designed to meet such requirements are targeted at oceans, with pixels on the order of 250–1000 m, far exceeding the spatial resolution needed for macrophyte mapping. Recent land-observing sensors such as Sentinel 2A/2B, SPOT 6/7, and Landsat 8 OLI have higher signal-to-noise ratios and improved calibration algorithms. Hence, mapping submerged macrophytes could become more feasible, although mapping individual species is likely still a continuing challenge without high spectral resolution data.

In summary, RS of aquatic IAS requires moderate to fine spatial resolution, high spectral resolution, and, for submerged IAS, high radiometric resolution. We are optimistic that future global mapping missions with climate-relevant mission durations can improve riparian and aquatic IAS mapping by enabling time-based

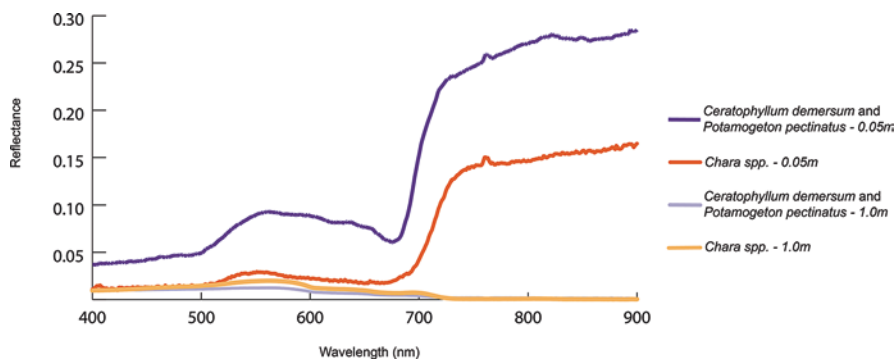


Fig. 12.8 Water column effects on reflectance of the submerged aquatic vegetation species hornwort (*Ceratophyllum demersum*), sago pondweed (*Potamogeton pectinatus*), and green algae (*Chara spp.*) from 5 cm water column height to 1 m water column height

approaches such as phenology signatures. Even without high spectral resolution data, RS of aquatic macrophytes is progressing. For example, through radiative transfer modeling, it has been shown to be robust for mapping aquatic macrophyte morphological traits in temperate systems (e.g., leaf area index, fractional cover, and biomass) across floating, emergent, and submerged macrophytes, which can be used to better quantify nutrient uptake, community dynamics, and invasion hotspots (Villa et al. 2014, 2015, 2017). The rapidly developing science of drone and UAS imagery also raises the potential to map IAS using differences in texture or using segmentation tools to do object-based mapping, especially when the area being mapped is small.

12.2.4 Agroecosystems

Agroecosystems are unique ecosystems due to the extraordinarily high anthropogenic interventions and pressures placed on them. Unlike other ecological systems, agricultural systems have more controlled environmental conditions with limited plant biodiversity. Crops are often grown as a monoculture, in uniform rows with highly regulated demography. Though crop species are often robust and herbicide resistant, many IAS are also developing resistance to herbicide, making them more invasive with increasing impacts on crops. With a rising global population, there is increased pressure on agricultural systems to increase productivity. IAS consume resources meant for crops and reduce yield, productivity, and income for farmers. In corn and soybean, two of the major crops grown in the United States losses due to IAS have been estimated at \$17 billion in soybean and \$27 billion in corn annually, approximately 50% of the yield of each of these crops (Soltani et al. 2016, 2017). IAS can become established in agroecosystems as in any other system, through both natural (wind, water, animals, forceful dehiscence) and artificial (machinery, crop seed, livestock feed, spreading of crop, and livestock waste) means. The application of water and nutrients also complicates the system by enhancing IAS' ability to compete with crops and reproduce. Often the effects of IAS depend on the crops present. Certain IAS may be problematic in some crops but not others due to crop management practices (time of planting, tillage, irrigation, mulch, registered herbicides, rotation).

To effectively detect IAS in agricultural systems, RS must meet the challenge of detecting IAS before they become competitive with crops. Field spectroscopy has been shown to be effective for discrimination of IAS from crops (Basinger 2018; Koger et al. 2004a, b; Gray et al. 2009), but it is not the most efficient due to the short duration of such field campaigns, since detection must then occur within a small window during one growing cycle. Research has long been published on the use of satellites or other airborne sensors for IAS detection in agriculture (Hunt et al. 2007; Menges et al. 1985), but these methods often lack the spatial and/or temporal resolution needed to detect IAS intermixed with a crop species.

One factor that aids in detection is that IAS tend to emerge in patches or patterns associated with farm management practices. For example, plants growing outside of the uniform row formations are often IAS and can be treated. Most studies typically investigate a single IAS. However, IAS are often intermixed, making them hard to distinguish from each other. Additionally, Basinger (2018) found that using field spectroscopy, IAS detection is not uniform across cropping systems and suggested that improved IAS detection may require crop-specific parameters for accurate IAS detection and control.

Hyperspectral data, as seen in Fig. 12.9, have also been demonstrated to enable detection of IAS density within the crop and determination of when in the planting cycle IAS are most readily detectable, especially during early growth stages (Basinger 2018). If only a few spectral bands are available, it can be very difficult to differentiate between species during the first few weeks after planting. So far, the most promising platform for IAS detection appears to be UAS. They have the necessary spatial resolution to locate IAS at early stages in the growing cycle, before they can spread or be obscured by the crop canopy, and UAS can be launched whenever necessary to collect imagery.

The main challenges of using RS in agroecosystems are associated with data latency (which impedes rapid IAS management on the part of producers) and the necessity of early growth cycle detection (where many species appear similar). Current market solutions tend to focus on active sensors or the use of artificial lighting rather than passive sensors. Commercial early IAS management systems used active proximal sensors to spot and spray IAS with herbicides. However, while

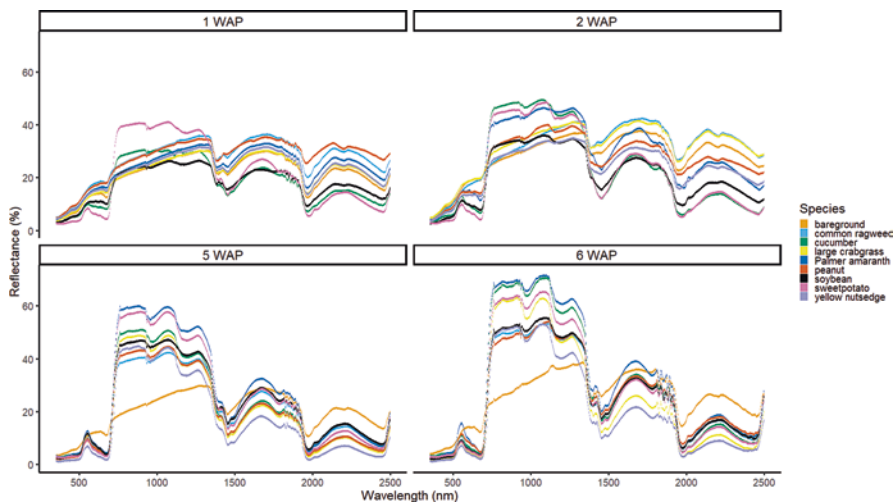


Fig. 12.9 Spectra of four crop species, cucumber (*Cucumis sativus*), peanut (*Arachis hypogaea*), soybean (*Glycine max*), and sweet potato (*Ipomoea batatas*), and four IAS, common ragweed (*Ambrosia artemisiifolia*), large crabgrass (*Digitaria sanguinalis*), Palmer amaranth (*Amaranthus palmeri*), and yellow nutsedge (*Cyperus esculentus*) over the first 10 weeks after being planted in 2016. (Data from Basinger (2018))

these systems can detect vegetation, they are not able to detect small IAS (Blackshaw et al. 1998) or distinguish between the crop and IAS. They thus rely solely on a priori assumptions about timing of emergence of IAS relative to crop species.

In summary, using RS in agroecosystems is only useful to growers within the timeline of crop cycles. IAS control is most effective when plants are small, but this is when they are also most difficult to detect and differentiate from the crop. IAS detection often requires high spatial and temporal resolution due to synchronous and asynchronous IAS emergence with the crop and sometimes high spectral resolution to deal with similar appearances during early growth stages. Implementing data-based management decisions is difficult if monitoring is not near constant due to the necessity of rapid responses. Thus, the use RS for the control of IAS has seen limited adoption in agriculture, despite a long history of research. However, UAS have become more common because the technology now meets several of the requirements for RS of IAS in agricultural settings.

12.2.5 Urban Ecosystems

More than half of all people live in urban areas, and this proportion is expected to increase substantially during this century. Urban ecosystems differ from agricultural or natural systems in terms of structural properties related to the built/natural ratio of the landscape; built area includes impervious and permeable built environments and the connecting infrastructure. Urban ecosystems have been colonized by increasing numbers of IAS (Paap et al. 2017; Hui et al. 2017). These ecosystems are unique because trees and other ornamental species in private and public city gardens are often non-native and can be sources of IAS to surrounding areas (Paap et al. 2017; Mayer-Pinto et al. 2017). IAS richness in urban areas is positively correlated with housing density (Gavier-Pizarro et al. 2010), urban wastelands (Bonthoux et al. 2014; Maurel et al. 2010), green infrastructure (Hostetler et al. 2011), and roads (Rupprecht et al. 2015). By harboring IAS, cities may unwittingly act as sources of IAS to surrounding agroecosystems and natural ecosystems (Paap et al. 2017; McLean et al. 2017).

Use of RS for IAS detection and mapping in urban environments is essential to gauge the affect of urban plants, which are often non-native, on the surrounding ecosystems. Detection has been successful with many forms of RS. For example, Shouse et al. (2012) used a combination of 0.3 m color aerial photographs and multispectral Landsat data to map bush honeysuckle (*Lonicera maackii*) under the forest canopy in an urban park in Louisville, Kentucky, USA. They conducted an object-based classification, a supervised classification, and constructed a species distribution model, with accuracies above 75%, especially for the object-based classification. This high accuracy can be attributed to extended greened-up seasons and high spatial resolution. Hyperspectral data has been used to detect Himalayan blackberry (*Rubus armeniacus*) and English ivy (*Hedera helix*) in nonforested areas of Surrey, British Columbia, Canada (Chance et al. 2016a). Classification accuracies

were higher than 75% for both; the potential for spectral separability was maximized by the choice of wavelength regions, and the researchers were able to increase accuracy using a random forest classifier, due to higher capability of under-canopy detection (Chance et al. 2016b). Because urban ecosystems are smaller than other ecosystems and more complex, high spatial resolution is necessary to detect IAS within the mostly non-vegetative ground cover.

Lidar with spectral data also has proven effective for mapping vegetation within urban areas. By combining lidar with hyperspectral imaging and a random forest classifier to map tree species including honey locust (*Gleditsia triacanthos*) in Surrey, British Columbia, Canada. Liu et al. (2017) further improved classification accuracy, showing the power of data fusion. Other studies have combined lidar data with IKONOS multispectral data to detect whether Chinese privet (*Ligustrum sinense*) invasion changed urban forest structure in Charlotte, North Carolina, USA (Singh et al. 2015). These researchers also found that a random forest built with lidar-derived metrics produced the best results.

RS of urban IAS, however, has some unique challenges. Because most of the ground is covered by manmade features, it is difficult to detect green areas and map and identify individual species (Alonzo et al. 2014). With sufficient spatial resolution, these challenges can be overcome. The most successful approach to date is to use a combination of hyperspectral and lidar, which yields spectral, structural, and height information.

In summary, detection of IAS in urban environments requires high spatial resolution to differentiate natural from built environments, high spectral resolution to identify species, and sufficient temporal resolution to detect IAS at different stages of invasion. While this is an emerging field with a growing literature, relatively few studies of IAS in urban environments have used RS data, and further research is needed in different geographical settings, invasion process phases, and urban density conditions.

12.3 Summary, Conclusions, and Prospectus

Invasive species are a major direct driver of biodiversity loss because they outcompete native species for local resources, eventually replacing or displacing them. They also cause indirect losses because they do not assume all of the ecological roles of the replaced native species. As they spread, IAS modify nutrient availability, nutrient cycling, soil chemistry, water quality, hydrology, food webs, habitats, and other ecosystem functions (Gordon 1998; Scheffer et al. 2003; Dukes and Mooney 2004; Hestir et al. 2016; Khanna et al. 2018), impairing ecosystem function. In addition to causing functional changes, IAS also modify ecosystem structure by physically changing canopy structures in forests and water quality in aquatic ecosystems. Increasing global changes related to climate, nutrient cycles, and land use will potentially change transport and introduction mechanisms of IAS in a way that provides a competitive advantage for new IAS, likely reducing effectiveness of

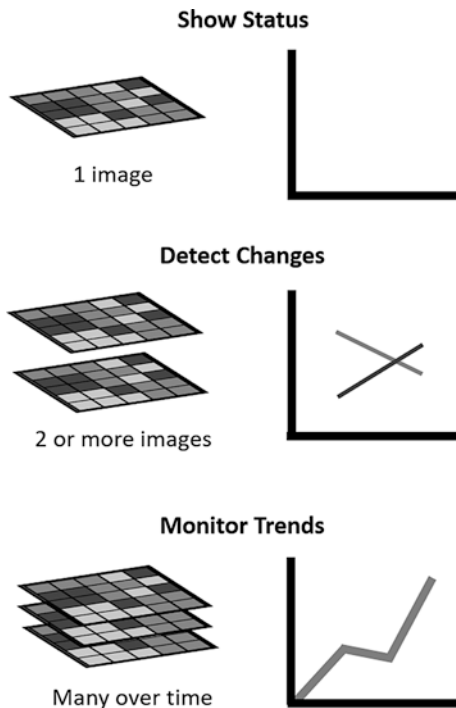
control strategies. The acceleration in global change and biodiversity loss degrades ecosystem resilience, threatening valuable ecosystem services. To preserve these services will require global cooperation on IAS monitoring and control with RS is a critical tool.

Each biome discussed in this chapter contains a unique complement of species. As a result, a different method of RS and data fusion works best for each. However, some methodologies can be valuable in all circumstances, such as increasing spectral information content. If only one IAS is of interest and it differs from its surroundings, multispectral data or use of photographs and texture analysis may be enough to identify and map it. However, in most cases there are multiple IAS competing with one another and with native vegetation, with varying canopy complexity and functional types. In such scenarios, difference in phenological characteristics can be exploited for identification. For example, an IAS might be identified through differing flowering times, flower colors, or earlier or later periods of senescence relative to surrounding vegetation. This requires temporally dense data. In cases where the invasion scenario is not simple or the data are not temporally sufficient, fusion between RS and other data sources (e.g., habitat models, DEMs, climate models) can be used to improve accuracy.

Data collection in the three domains of RS (spectral, spatial, and temporal) can be optimized for a species based on the ecosystem type and image analysis approach. For forests, lidar data are often a good addition to spectral information because they can provide information on height and physical crown structure. For species below the forest canopy, indirect methods such as models based on ecological knowledge of the species may be necessary, or imagery may simply be collected during a leaf-off period. IAS in grasslands often have similar spectral properties to natives, requiring hyperspectral data, strategic image timing, or indirect modeling methods. Aquatic ecosystems introduce many confounding factors due to presence of water and its associated processes, necessitating high radiometric quality and good calibration. Because this biome is so complex, hyperspectral information and customized image timing are a must for differentiating IAS. Additionally, radiative transfer modeling is often necessary to detect submerged and water column IAS. Agroecosystems have minimal diversity, so fewer spectral data are required. However, frequent assessment is necessary to allow a timely response to minimize crop loss. RS detection of IAS in urban ecosystems requires varying methods and unique adaptations because of the high potential for introductions and unusual landscape features, such as impervious surfaces.

These factors underscore the importance of mission design for two key data collection platforms. First, airborne platforms (piloted and unpiloted), which are vital to rapid, local-scale assessments, must acquire data at key times relevant to IAS phenology. As temperatures and biodiversity losses continue to increase, plant phenology is expected to continue to change (Primack et al. 2015; Wolf et al. 2017) and airborne acquisition strategies must adjust accordingly. Second, satellite platforms are critical to providing global-scale systematic monitoring of IAS. Current and future missions must include high spectral resolution sensors with the capability to create climate-relevant time series (a duration on the order of approximately a

Fig. 12.10 Accumulation of RS data over time makes RS a powerful tool for monitoring and understanding the spread of IAS, as well as filling an important role in IAS management. (Image credit: Vanessa Tobias, California Department of Fish and Wildlife)



decade) to characterize phenology for widespread IAS detection, particularly for grasslands and forests (Fig. 12.10).

To date, most IAS management has been reactive. RS can help land managers see where IAS occur, target removal, monitor rates of growth and expansion, and evaluate treatment effectiveness. The future of the field is in prevention. Novel research is starting to focus on invasion processes, impacts, and management assessments (e.g., Santos et al. 2009; Hestir et al. 2016; Santos et al. 2016). Further research is needed to understand how RS can be fully integrated into understanding the invasion process, from arrival to establishment and spread. Freely available time series data alongside increasing amounts of field data related to early detection of IAS may allow the achievement of such a goal. For this reason, it is important to cultivate a cross-disciplinary understanding of the invasion process and the effects IAS on ecosystems and biodiversity. Two promising developments that will increase support for IAS mapping and monitoring are the upcoming Surface Biology and Geology (SBG) global mapping hyperspectral satellite (Schimel, Chap. 19) and the use of UAS imaging spectroscopy. The new satellite offers potential to improve mapping of IAS on a global scale; though limited by spatial resolution, it will still be capable of species level identification in many situations. UAS offer high spatial resolution mapping on demand, providing flexibility and simplification of RS missions, reducing costs compared with manned flights, and improving safety. These two developments will drastically improve the volume of data being collected and, with scientific innovation, help minimize economic and environmental impacts of IAS (Fig. 12.11).

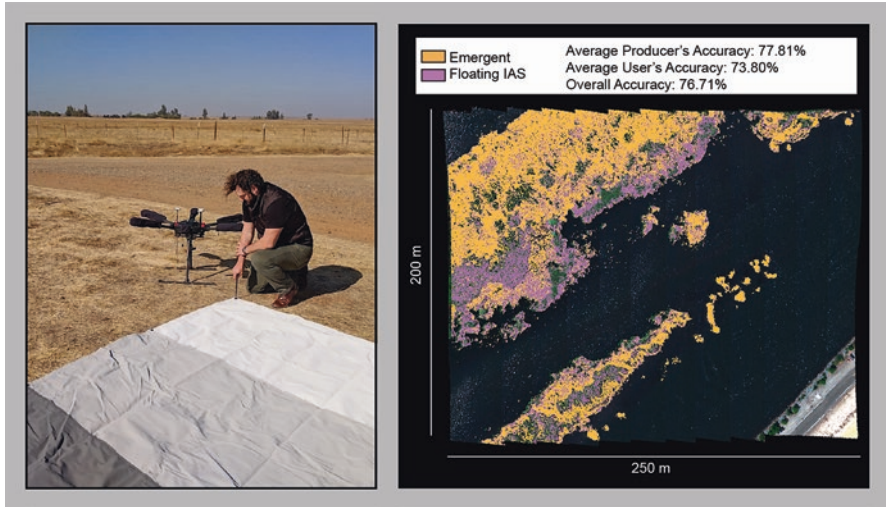


Fig. 12.11 New off the shelf UAS systems offer hyperspectral image collection, providing new capabilities, and presenting new challenges. This image shows a preliminary classification of floating IAS and emergent vegetation overlaid on top of an RGB flightline mosaic. The flight took approximately 20 min to cover a 250 m × 200 m area with 5.5 cm spatial resolution. Raw data size for all of the flightlines is roughly 40 gb

References

- Ackleson SG, Klemas V (1987) Remote sensing of submerged aquatic vegetation in lower Chesapeake Bay: a comparison of Landsat MSS to TM imagery. *Remote Sens Environ* 22:235–248. [https://doi.org/10.1016/0034-4257\(87\)90060-5](https://doi.org/10.1016/0034-4257(87)90060-5)
- Albright TP, Moorhouse TG, Mcnabb TJ (2004) The rise and fall of water hyacinth in Lake Victoria and the Kagera river basin. *J Aquat Plant Manage* 42:73–84
- Ali I, Cawkwell F, Dwyer E et al (2016) Satellite remote sensing of grasslands: from observation to management. *J Plant Ecol* 9:649–671. <https://doi.org/10.1093/jpe/rtw005>
- Allen JM, Bradley BA (2016) Out of the weeds? Reduced plant invasion risk with climate change in the continental United States. *Biol Conserv* 203:306–312. <https://doi.org/10.1016/j.biocon.2016.09.015>
- Alonzo M, Bookhagen B, Roberts DA (2014) Urban tree species mapping using hyperspectral and lidar data fusion. *Remote Sens Environ* 148:70–83. <https://doi.org/10.1016/j.rse.2014.03.018>
- Amaral CH, Roberts DA, Almeida TIR, Souza Filho CR (2015) Mapping invasive species and spectral mixture relationships with neotropical woody formations in southeastern Brazil. *ISPRS J Photogramm Remote Sens* 108:80–93. <https://doi.org/10.1016/j.isprsjprs.2015.06.009>
- Anderson JM (1991) The effects of climate change on decomposition processes in grassland and coniferous forests. *Ecol Appl* 1:326–347. <https://doi.org/10.2307/1941761>
- Anderson GL, Hanson JD, Haas RH (1993) Evaluating landsat thematic mapper derived vegetation indices for estimating above-ground biomass on semiarid rangelands. *Remote Sens Environ* 45:165–175. [https://doi.org/10.1016/0034-4257\(93\)90040-5](https://doi.org/10.1016/0034-4257(93)90040-5)
- Anderson DM, Glibert PM, Burkholder JM (2002) Harmful algal blooms and eutrophication: nutrient sources, composition, and consequences. *Estuaries* 25:704–726. <https://doi.org/10.1007/bf02804901>

- Andrew ME, Ustin SL (2008) The role of environmental context in mapping invasive plants with hyperspectral image data. *Remote Sens Environ* 112:4301–4317. <https://doi.org/10.1016/j.rse.2008.07.016>
- Andrew ME, Ustin SL (2009) Habitat suitability modelling of an invasive plant with advanced remote sensing data. *Divers Distrib* 15:627–640. <https://doi.org/10.1111/j.1472-4642.2009.00568.x>
- Arzandeh S, Wang J (2003) Monitoring the change of phragmites distribution using satellite data. *Can J Remote Sens* 29:24–35. <https://doi.org/10.5589/m02-077>
- Asner GP, Jones MO, Martin RE et al (2008a) Remote sensing of native and invasive species in Hawaiian forests. *Remote Sens Environ* 112:1912–1926. <https://doi.org/10.1016/j.rse.2007.02.043>
- Asner GP, Knapp DE, Kennedy-Bowdoin T et al (2008b) Invasive species detection in Hawaiian rainforests using airborne imaging spectroscopy and LiDAR. *Remote Sens Environ* 112:1942–1955. <https://doi.org/10.1016/j.rse.2007.11.016>
- Balch JK, Bradley BA, D'Antonio CM, Gómez-Dans J (2013) Introduced annual grass increases regional fire activity across the arid western USA (1980–2009). *Glob Chang Biol* 19:173–183. <https://doi.org/10.1111/gcb.12046>
- Barbier EB, Hacker SD, Kennedy C et al (2011) The value of estuarine and coastal ecosystem services. *Ecol Monogr* 81:169–193. <https://doi.org/10.1890/10-1510.1>
- Barbosa JM, Asner GP, Martin RE et al (2016) Determining subcanopy *Psidium cattleianum* invasion in Hawaiian forests using imaging spectroscopy. *Remote Sens* 8:33. <https://doi.org/10.3390/rs8010033>
- Basinger NT (2018) Interference and spectral changes of Palmer Amaranth (*Amaranthus palmeri* S. Wats.) and large crabgrass (*Digitaria sanguinalis* (L.) Scop.) density in sweet potato and soybean and use of spectroscopy for discrimination of crop and weed species. Dissertation, North Carolina State University
- Bellard C, Thuiller W, Leroy B et al (2013) Will climate change promote future invasions? *Glob Chang Biol* 19:3740–3748. <https://doi.org/10.1111/gcb.12344>
- Blackshaw RE, Molnar LJ, Lindwall CW (1998) Merits of a weed-sensing sprayer to control weeds in conservation fallow and cropping systems. *Weed Sci* 46:120–126
- Bonthoux S, Brun M, Di Pietro F et al (2014) How can wastelands promote biodiversity in cities? A review. *Landsc Urban Plan* 132:79–88. <https://doi.org/10.1016/j.landurbplan.2014.08.010>
- Boschetti M, Boschetti L, Oliveri S et al (2007) Tree species mapping with airborne hyperspectral MIVIS data: the Ticino Park study case. *Int J Remote Sens* 28:1251–1261. <https://doi.org/10.1080/01431160600928542>
- Bostater CR Jr, Ghir T, Bassetti L et al (2004) Hyperspectral remote sensing protocol development for submerged aquatic vegetation in shallow waters. In: *Remote sensing of the ocean and sea ice 2003*. International Society for Optics and Photonics, pp 199–216
- Boyte SP, Wylie BK (2017) A time series of herbaceous annual cover in the sagebrush ecosystem. U.S. Geological Survey data release. <https://doi.org/10.5066/F71J98QK>
- Boyte SP, Wylie BK, Major DJ (2015) Mapping and monitoring cheatgrass dieoff in rangelands of the northern Great Basin, USA. *Rangel Ecol Manag* 68:18–28. <https://doi.org/10.1016/j.rama.2014.12.005>
- Bracher A, Bouman HA, Brewin RJW et al (2017) Obtaining phytoplankton diversity from ocean color: a scientific roadmap for future development. *Front Mar Sci* 4:55. <https://doi.org/10.3389/fmars.2017.00055>
- Bradley BA (2014) Remote detection of invasive plants: a review of spectral, textural and phenological approaches. *Biol Invasions* 16:1411–1425. <https://doi.org/10.1007/s10530-013-0578-9>
- Bradley BA, Mustard JF (2008) Comparison of phenology trends by land cover class: a case study in the Great Basin, USA. *Glob Chang Biol* 14:334–346. <https://doi.org/10.1111/j.1365-2486.2007.01479.x>
- Bradley BA, Blumenthal DM, Wilcove DS, Ziska LH (2010) Predicting plant invasions in an era of global change. *Trends Ecol Evol* 25:310–318. <https://doi.org/10.1016/j.tree.2009.12.003>
- Brooks ML, D'Antonio CM, Richardson DM et al (2004) Effects of invasive alien plants on fire regimes. *Bioscience* 54:677. [https://doi.org/10.1641/0006-3568\(2004\)054\[0677:EOIAP0\]2.0.CO;2](https://doi.org/10.1641/0006-3568(2004)054[0677:EOIAP0]2.0.CO;2)

- Brown SD, Dooling RJ (1993) Perception of conspecific faces by budgerigars (*Melopsittacus undulatus*): II. Synthetic models. *J Comp Psychol* 107:48–60. <https://doi.org/10.1037/0735-7036.107.1.48>
- Byers JE, Noonburg EG (2003) Scale dependent effects of biotic resistance to biological invasion. *Ecology* 84:1428–1433. <https://doi.org/10.1890/02-3131>
- Campbell BM (ed) (1996) *The Miombo in transition: woodlands and welfare in Africa*. CIFOR, Bogor, Indonesia
- Carter GA, Lucas KL, Blossom GA et al (2009) Remote sensing and mapping of tamarisk along the Colorado River, USA: a comparative use of summer-acquired Hyperion, Thematic Mapper and QuickBird data. *Remote Sens* 1:318–329. <https://doi.org/10.3390/rs1030318>
- Cavalli RM, Laneve G, Fusilli L et al (2009) Remote sensing water observation for supporting Lake Victoria weed management. *J Environ Manag* 90:2199–2211. <https://doi.org/10.1016/j.jenvman.2007.07.036>
- Chance CM, Coops NC, Crosby K, Aven N (2016a) Spectral wavelength selection and detection of two invasive plant species in an urban area. *Can J Remote Sens* 42:27–40. <https://doi.org/10.1080/07038992.2016.1143330>
- Chance CM, Coops NC, Plowright AA et al (2016b) Invasive shrub mapping in an urban environment from hyperspectral and LiDAR-derived attributes. *Front Plant Sci* 07:1528
- Chen Z, Hu C, Muller-Karger FE, Luther ME (2010) Short-term variability of suspended sediment and phytoplankton in Tampa Bay, Florida: observations from a coastal oceanographic tower and ocean color satellites. *Estuar Coast Shelf Sci* 89:62–72. <https://doi.org/10.1016/j.ecss.2010.05.014>
- Cheng Y-B, Tom E, Ustin SL (2007) Mapping an invasive species, kudzu (*Pueraria montana*), using hyperspectral imagery in western Georgia. *J Appl Remote Sens* 1:013514. <https://doi.org/10.1117/1.2749266>
- Convention on Biological Diversity (CBD) (2010) Year in review. Secretariat of the Convention on Biological Diversity, Montreal, p 2009
- Cuneo P, Jacobson CR, Leishman MR (2009) Landscape-scale detection and mapping of invasive African Olive (*Olea europaea* L. ssp. *cuspidata* Wall ex G. Don Ciferri) in SW Sydney, Australia using satellite remote sensing. *Appl Veg Sci* 12:145–154. <https://doi.org/10.1111/j.1654-109X.2009.01010.x>
- D'Antonio CM, Vitousek PM (1992) Biological invasions by exotic grasses, the grass/fire cycle, and global change. *Annu Rev Ecol Syst* 23:63–87. <https://doi.org/10.1146/annurev.es.23.110192.000431>
- Derner JD, Schuman GE (2007) Carbon sequestration and rangelands: a synthesis of land management and precipitation effects. *J Soil Water Conserv* 62:77–85
- Diao C, Wang L (2016) Incorporating plant phenological trajectory in exotic saltcedar detection with monthly time series of Landsat imagery. *Remote Sens Environ* 182:60–71. <https://doi.org/10.1016/j.rse.2016.04.029>
- Dierssen H, McManus GB, Chlus A et al (2015) Space station image captures a red tide ciliate bloom at high spectral and spatial resolution. *Proc Natl Acad Sci* 112:14783–14787
- Dogan OK, Akyurek Z, Beklioglu M (2009) Identification and mapping of submerged plants in a shallow lake using QuickBird satellite data. *J Environ Manag* 90:2138–2143. <https://doi.org/10.1016/j.jenvman.2007.06.022>
- Dörnhöfer K, Oppelt N (2016) Remote sensing for lake research and monitoring - recent advances. *Ecol Indic* 64:105–122. <https://doi.org/10.1016/j.ecolind.2015.12.009>
- Downs J, Larson K, Cullinan V (2016) Mapping cheatgrass across the range of the greater sage-grouse: linking biophysical, climate and remote sensing data to predict cheatgrass occurrence. Pacific Northwest National Laboratory. https://static1.squarespace.com/static/5016c7a324ac93bdfdfb930c/t/582b58e746c3c44fc1e27c19/1479235820777/2016_9MappingCheatgrassSageGrouseRange.pdf. Accessed 30 Nov 2018
- Dudgeon D, Arthington AH, Gessner MO et al (2015) Freshwater biodiversity: importance, threats, status and conservation challenges. *Society* 81:163–182. <https://doi.org/10.1017/S1464793105006950>

- Dukes JS, Mooney HA (1999) Does global change increase the success of biological invaders? *Trends Ecol Evol* 14:135–139. [https://doi.org/10.1016/S0169-5347\(98\)01554-7](https://doi.org/10.1016/S0169-5347(98)01554-7)
- Dukes JS, Mooney HA (2004) Disruption of ecosystem processes in western North America by invasive species. *Rev Chil Hist Nat* 77:411–437. <https://doi.org/10.4067/S0716-078X2004000300003>
- European Environmental Agency (EEA) (2012) Invasive alien species indicators in Europe – a review of streamlining European biodiversity (SEBI) indicator 10. EEA Technical Report No 15/2012. European Environment Agency, Copenhagen
- Evangelista PH, Stohlgren TJ, Morisette JT, Kumar S (2009) Mapping invasive tamarisk (*Tamarix*): a comparison of single-scene and time-series analyses of remotely sensed data. *Remote Sens* 1:519–533. <https://doi.org/10.3390/rs1030519>
- Everitt JH, Pettit RD, Alaniz MA (1987) Remote sensing of broom snakeweed (*Gutierrezia sarothrae*) and spiny aster (*Aster spinosus*). *Weed Sci* 35:295–302
- Everitt JH, Anderson GL, Escobar DE et al (1995) Use of remote-sensing for detecting and mapping leafy spurge (*Euphorbia-Esula*). *Weed Technol* 9:599–609. <https://doi.org/10.1017/s0890037x00023915>
- Everitt JH, Yang C, Escobar DE et al (1999) Using remote sensing and spatial information technologies to detect and map two aquatic macrophytes. *J Aquat Plant Manag* 37:71–80
- Everitt JH, Yang C, Flores DG (2003) Light reflectance characteristics and remote sensing of waterlettuce. *J Aquat Plant Manag* 41:39–44. <https://doi.org/10.2307/4003041>
- Everitt JH, Yang C, Summy KR et al (2011) Evaluation of hyperspectral reflectance data for discriminating six aquatic weeds. *J Aquat Plant Manag* 49:94–100
- Finlayson MC (2012) Forty years of wetland conservation and wise use. *Aquat Conserv Mar Freshw Ecosyst* 22:139–143. <https://doi.org/10.1002/aqc.2233>
- Foley JA, Asner GP, Costa MH et al (2007) Amazonia revealed: forest degradation and loss of ecosystem goods and services in the Amazon Basin. *Front Ecol Environ* 5:25–32. [https://doi.org/10.1890/1540-9295\(2007\)5\[25:arfdal\]2.0.co;2](https://doi.org/10.1890/1540-9295(2007)5[25:arfdal]2.0.co;2)
- Fuller DO (2005) Remote detection of invasive melaleuca trees (*Melaleuca quinquenervia*) in South Florida with multispectral IKONOS imagery. *Int J Remote Sens* 26:1057–1063. <https://doi.org/10.1080/01430060512331314119>
- Gamon JA, Serrano L, Surfus JS (1997) International association for ecology the photochemical reflectance index: an optical indicator of photosynthetic radiation use efficiency across species, functional types, and nutrient levels. *Oecologia* 112:492–501
- Gao B-C (1995) Normalized difference water index for remote sensing of vegetation liquid water from space. In: *Imaging spectrometry*, Orlando, June 1995, vol 2480, SPIE (International Society for Optics and Photonics), pp 225–237. <https://doi.org/10.1117/12.210877>
- Gavier-Pizarro GI, Radeloff VC, Stewart SI et al (2010) Housing is positively associated with invasive exotic plant species richness in New England, USA. *Ecol Appl* 20:1913–1925. <https://doi.org/10.1890/09-2168.1>
- Gherardi F (2007) Biological invasions in inland waters: an overview. In: *Biological invaders in inland waters: profiles, distribution, and threats*. Springer Netherlands, Dordrecht, pp 3–25
- Giardino C, Bresciani M, Villa P, Martinelli A (2010) Application of remote sensing in water resource management: the case study of Lake Trasimeno, Italy. *Water Resour Manag* 24:3885–3899. <https://doi.org/10.1007/s11269-010-9639-3>
- Giardino C, Candiani G, Bresciani M et al (2012) BOMBER: a tool for estimating water quality and bottom properties from remote sensing images. *Comput Geosci* 45:313–318. <https://doi.org/10.1016/j.cageo.2011.11.022>
- Giardino C, Brando VE, Gege P et al (2018) Imaging spectrometry of inland and coastal waters: state of the art, achievements and perspectives. *Surv Geophys* 40:1–29. <https://doi.org/10.1007/s10712-018-9476-0>
- Glenn NF, Mundt JT, Weber KT et al (2005) Hyperspectral data processing for repeat detection of small infestations of leafy spurge. *Remote Sens Environ* 95:399–412. <https://doi.org/10.1016/j.rse.2005.01.003>

- Gordon DR (1998) Effects of invasive, non-indigenous plant species on ecosystem processes: lessons from Florida. *Ecol Appl* 8:975. <https://doi.org/10.2307/2640955>
- Grace J, José JS, Meir P et al (2006) Productivity and carbon fluxes of tropical savannas. *J Biogeogr* 33:387–400. <https://doi.org/10.1111/j.1365-2699.2005.01448.x>
- Gray CJ, Shaw DR, Bruce LM (2009) Utility of hyperspectral reflectance for differentiating soybean (*Glycine max*) and six weed species. *Weed Technol* 23:108–119. <https://doi.org/10.1614/WT-07-117.1>
- Hamada Y, Stow DA, Coulter LL et al (2007) Detecting tamarisk species (*Tamarix spp.*) in riparian habitats of southern California using high spatial resolution hyperspectral imagery. *Remote Sens Environ* 109:237–248. <https://doi.org/10.1016/j.rse.2007.01.003>
- Hantson W, Kooistra L, Slim PA (2012) Mapping invasive woody species in coastal dunes in the Netherlands: a remote sensing approach using LIDAR and high-resolution aerial photographs. *Appl Veg Sci* 15:536–547. <https://doi.org/10.1111/j.1654-109X.2012.01194.x>
- He KS, Rocchini D, Neteler M, Nagendra H (2011) Benefits of hyperspectral remote sensing for tracking plant invasions. *Divers Distrib* 17:381–392. <https://doi.org/10.1111/j.1472-4642.2011.00761.x>
- He KS, Bradley BA, Cord AF et al (2015) Will remote sensing shape the next generation of species distribution models? *Remote Sens Ecol Conserv* 1:4–18. <https://doi.org/10.1002/rse2.7>
- Hellmann JJ, Byers JE, Bierwagen BG, Dukes JS (2008) Five potential consequences of climate change for invasive species. *Conserv Biol* 22:534–543. <https://doi.org/10.1111/j.1523-1739.2008.00951.x>
- Hestir EL, Khanna S, Andrew ME et al (2008) Identification of invasive vegetation using hyperspectral remote sensing in the California Delta ecosystem. *Remote Sens Environ* 112:4034–4047. <https://doi.org/10.1016/j.rse.2008.01.022>
- Hestir EL, Greenberg JA, Ustin SL (2012) Classification trees for aquatic vegetation community prediction from imaging spectroscopy. *IEEE J Sel Top Appl Earth Obs Remote Sens* 5:1572–1584. <https://doi.org/10.1109/jstars.2012.2200878>
- Hestir EL, Brando VE, Bresciani M et al (2015) Measuring freshwater aquatic ecosystems: the need for a hyperspectral global mapping satellite mission. *Remote Sens Environ* 167:181–195. <https://doi.org/10.1016/j.rse.2015.05.023>
- Hestir EL, Schoellhamer DH, Greenberg J et al (2016) The effect of submerged aquatic vegetation expansion on a declining turbidity trend in the Sacramento-San Joaquin River Delta. *Estuar Coasts* 39:1100–1112. <https://doi.org/10.1007/s12237-015-0055-z>
- Hostetler M, Allen W, Meurk C (2011) Conserving urban biodiversity? Creating green infrastructure is only the first step. *Landsc Urban Plan* 100:369–371. <https://doi.org/10.1016/j.landurbplan.2011.01.011>
- Hoyos LE, Gavier-Pizarro GI, Kuemmerle T et al (2010) Invasion of glossy privet (*Ligustrum lucidum*) and native forest loss in the Sierras Chicas of Córdoba, Argentina. *Biol Invasions* 12:3261–3275. <https://doi.org/10.1007/s10530-010-9720-0>
- Hu S, Niu Z, Chen Y et al (2017) Global wetlands: potential distribution, wetland loss, and status. *Sci Total Environ* 586:319–327. <https://doi.org/10.1016/j.scitotenv.2017.02.001>
- Huang CY, Asner GP (2009) Applications of remote sensing to alien invasive plant studies. *Sensors (Switzerland)* 9:4869–4889. <https://doi.org/10.3390/s90604869>
- Huang CY, Geiger EL (2008) Climate anomalies provide opportunities for large-scale mapping of non-native plant abundance in desert grasslands. *Divers Distrib* 14:875–884. <https://doi.org/10.1111/j.1472-4642.2008.00500.x>
- Hudak AT, Wessman CA (1998) Textural analysis of historical aerial photography to characterize woody plant encroachment in South African Savanna. *Remote Sens Environ* 66:317–330. [https://doi.org/10.1016/S0034-4257\(98\)00078-9](https://doi.org/10.1016/S0034-4257(98)00078-9)
- Hui C, Richardson DM, Visser V (2017) Ranking of invasive spread through urban green areas in the world's 100 most populous cities. *Biol Invasions* 19:3527–3539. <https://doi.org/10.1007/s10530-017-1584-0>
- Hulme PE (2009) Trade, transport and trouble: managing invasive species pathways in an era of globalization. *J Appl Ecol* 46:10–18. <https://doi.org/10.1111/j.1365-2664.2008.01600.x>

- Hulme PE (2015) Invasion pathways at a crossroad: policy and research challenges for managing alien species introductions. *J Appl Ecol* 52:1418–1424. <https://doi.org/10.1111/1365-2664.12470>
- Hunt ER, Daughtry CST, Kim MS, Williams AEP (2007) Using canopy reflectance models and spectral angles to assess potential of remote sensing to detect invasive weeds. *J Appl Remote Sens* 1:013506. <https://doi.org/10.1117/1.2536275>
- Hunter PD, Gilvear DJ, Tyler AN et al (2010) Mapping macrophytic vegetation in shallow lakes using the compact airborne spectrographic imager (CASI). *Aquat Conserv Mar Freshw Ecosyst* 20:717–727. <https://doi.org/10.1002/aqc.1144>
- Ingwell LL, Bosque-Pérez NA (2015) The invasive weed *Ventenata dubia* is a host of *Barley yellow dwarf virus* with implications for an endangered grassland habitat. *Weed Res* 55:62–70. <https://doi.org/10.1111/wre.12110>
- Ishii J, Washitani I (2013) Early detection of the invasive alien plant *Solidago altissima* in moist tall grassland using hyperspectral imagery. *Int J Remote Sens* 34:5926–5936. <https://doi.org/10.1080/01431161.2013.799790>
- Jenkerson CB, Maiersperger T, Schmidt G (2010) eMODIS: a user-friendly data source. US Geological Survey. <https://doi.org/10.3133/ofr20101055>
- Jollineau MY, Howarth PJ (2008) Mapping an inland wetland complex using hyperspectral imagery. *Int J Remote Sens* 29:3609–3631. <https://doi.org/10.1080/01431160701469099>
- Joshi C, De Leeuw J, Van Andel J et al (2006) Indirect remote sensing of a cryptic forest understorey invasive species. *For Ecol Manag* 225:245–256. <https://doi.org/10.1016/j.foreco.2006.01.013>
- Junk WJ, Bayley PB, Sparks RE (1989) The flood-pulse concept in river-floodplain systems. *Proc Int Large River Symp Can Spec Publ Fish Aquat Sci* 106:110–127
- Keane RM, Crawley MJ (2002) Exotic plant invasions and the enemy release hypothesis. *Trends Ecol Evol* 17:164–170. [https://doi.org/10.1016/S0169-5347\(02\)02499-0](https://doi.org/10.1016/S0169-5347(02)02499-0)
- Khanna S, Santos MJ, Ustin SL, Haverkamp PJ (2011) An integrated approach to a biophysically based classification of floating aquatic macrophytes. *Int J Remote Sens* 32:1067–1094. <https://doi.org/10.1080/01431160903505328>
- Khanna S, Santos MJ, Boyer JD et al (2018) Water primrose invasion changes successional pathways in an estuarine ecosystem. *Ecosphere* 9(9). <https://doi.org/10.1002/ecs2.2418>
- Kimothi MM, Anitha D, Vasistha HB et al (2010) Remote sensing to map the invasive weed, *Lantana camara* in forests. *Trop Ecol* 51:67–74
- Koger CH, Shaw DR, Reddy KN, Bruce LM (2004a) Detection of pitted morningglory (*Ipomoea lacunosa*) with hyperspectral remote sensing. I. Effects of vegetation ground cover and reflectance properties. *Weed Sci* 52:230–235. <https://doi.org/10.1614/ws-03-083r1>
- Koger CH, Shaw DR, Reddy KN, Bruce LM (2004b) Detection of pitted morningglory (*Ipomoea lacunosa*) with hyperspectral remote sensing. II. Effects of vegetation ground cover and reflectance properties. *Weed Sci* 52:230–235. <https://doi.org/10.1614/ws-03-083r1>
- Kudela RM, Palacios SL, Austerberry DC et al (2015) Application of hyperspectral remote sensing to cyanobacterial blooms in inland waters. *Remote Sens Environ* 167:196–205. <https://doi.org/10.1016/j.rse.2015.01.025>
- Laba M, Tsai F, Ogurcak D et al (2005) Field determination of optimal dates for the discrimination of invasive wetland plant species using derivative spectral analysis. *Photogramm Eng Remote Sensing* 71:603–611. <https://doi.org/10.14358/pers.71.5.603>
- Laba M, Downs R, Smith S et al (2008) Mapping invasive wetland plants in the Hudson River National Estuarine Research Reserve using QuickBird satellite imagery. *Remote Sens Environ* 112:286–300. <https://doi.org/10.1016/j.rse.2007.05.003>
- Landmann T, Piironen R, Makori DM et al (2015) Application of hyperspectral remote sensing for flower mapping in African savannas. *Remote Sens Environ* 166:50–60. <https://doi.org/10.1016/j.rse.2015.06.006>
- Lass LW, Prather TS (2004) Detecting the locations of Brazilian pepper trees in the everglades with a hyperspectral sensor. *Weed Technol* 18:437–442. <https://doi.org/10.1614/wt-03-174r>
- Lass LW, Thill DC, Shafii B, Prather TS (2002) Detecting spotted knapweed (*Centaurea maculosa*) with hyperspectral remote sensing technology. *Weed Technol* 16:426–432. [https://doi.org/10.1614/0890-037x\(2002\)016\[0426:dkcmw\]2.0.co;2](https://doi.org/10.1614/0890-037x(2002)016[0426:dkcmw]2.0.co;2)

- Lass LW, Prather TS, Glenn NF et al (2005) A review of remote sensing of invasive weeds and example of the early detection of spotted knapweed (*Centaurea maculosa*) and babysbreath (*Gypsophila paniculata*) with a hyperspectral sensor. *Weed Sci* 53:242–251. <https://doi.org/10.1614/ws-04-044r2>
- Latham J, Cumani R, Rosati I, Bloise M (2014) Global Land Cover SHARE (GLC-SHARE) database Beta-Release Version 1.0
- Latombe G, Pyšek P, Jeschke JM et al (2017) A vision for global monitoring of biological invasions. *Biol Conserv* 213:295–308. <https://doi.org/10.1016/j.biocon.2016.06.013>
- Lawrence RL, Wood SD, Sheley RL (2006) Mapping invasive plants using hyperspectral imagery and Breiman Cutler classifications (randomForest). *Remote Sens Environ* 100:356–362. <https://doi.org/10.1016/j.rse.2005.10.014>
- Levine JM (2000) Species diversity and biological invasions: relating local process to community pattern. *Science* 288:852–854. <https://doi.org/10.1126/science.288.5467.852>
- Liu L, Coops NC, Aven NW, Pang Y (2017) Mapping urban tree species using integrated airborne hyperspectral and LiDAR remote sensing data. *Remote Sens Environ* 200:170–182. <https://doi.org/10.1016/j.rse.2017.08.010>
- Lowe S, Browne M, Boudjelas S, De Poorter M (2000) 100 of the world's worst invasive alien species: a selection from the global invasive species database. Invasive Species Specialist Group, Auckland
- Lymburner L, Botha E, Hestir E et al (2016) Landsat 8: providing continuity and increased precision for measuring multi-decadal time series of total suspended matter. *Remote Sens Environ* 185:108–118. <https://doi.org/10.1016/j.rse.2016.04.011>
- Maheu-Giroux M, De Blois S (2005) Mapping the invasive species *Phragmites australis* in linear wetland corridors. *Aquat Bot* 83:310–320. <https://doi.org/10.1016/j.aquabot.2005.07.002>
- Malthus TJ, George DG (1997) Airborne remote sensing of macrophytes in Cefni Reservoir, Anglesey, UK. *Aquat Bot* 58:317–332. [https://doi.org/10.1016/S0304-3770\(97\)00043-0](https://doi.org/10.1016/S0304-3770(97)00043-0)
- Malthus TJ, Hestir EL, Dekker AG, Brando VE (2012) The case for a global inland water quality product. In: 2012 IEEE international geoscience and remote sensing symposium (IGARSS), Munich, July 2012. pp 5234–5237. <https://doi.org/10.1109/igarss.2012.6352429>
- Marshall TR, Lee PF (1994). Mapping aquatic macrophytes through digital image analysis of aerial photographs: an assessment. *J Aquat Plant Manag*, 32:61–66
- Masters G, Norgrove L (2010) Climate change and invasive alien species. UK CABI Work Pap 1. <https://www.cabi.org/Uploads/CABI/expertise/invasive-alien-species-working-paper.pdf>. Accessed 3 Dec 2018
- Matthews MW (2011) A current review of empirical procedures of remote sensing in inland and near-coastal transitional waters. *Int J Remote Sens* 32:6855–6899. <https://doi.org/10.1080/01431161.2010.512947>
- Maurel N, Salmon S, Ponge JF et al (2010) Does the invasive species *Reynoutria japonica* have an impact on soil and flora in urban wastelands? *Biol Invasions* 12:1709–1719. <https://doi.org/10.1007/s10530-009-9583-4>
- Mayer-Pinto M, Johnston EL, Bugnot AB et al (2017) Building 'blue': an eco-engineering framework for foreshore developments. *J Environ Manag* 189:109–114. <https://doi.org/10.1016/j.jenvman.2016.12.039>
- McIntyre K, McLaren K, Prospere K (2018) Mapping shallow nearshore benthic features in a Caribbean marine-protected area: assessing the efficacy of using different data types (hydroacoustic versus satellite images) and classification techniques. *Int J Remote Sens* 39:1117–1150. <https://doi.org/10.1080/01431161.2017.1395924>
- McLean P, Gallien L, Wilson JRJ et al (2017) Small urban centres as launching sites for plant invasions in natural areas: insights from South Africa. *Biol Invasions* 19:3541–3555. <https://doi.org/10.1007/s10530-017-1600-4>
- Menges RM, Nixon PR, Richardson AJ (1985) Light reflectance and remote sensing of weeds in agronomic and horticultural crops. *Weed Sci* 33:569–581. <https://doi.org/10.2307/4044150>
- Mertes LAK, Smith MO, Adams JB (1993) Estimating suspended sediment concentrations in surface waters of the Amazon River wetlands from Landsat images. *Remote Sens Environ* 43:281–301. [https://doi.org/10.1016/0034-4257\(93\)90071-5](https://doi.org/10.1016/0034-4257(93)90071-5)

- Mitchell JJ, Glenn NF (2009) Leafy spurge (*Euphorbia esula*) classification performance using hyperspectral and multispectral sensors. *Rangel Ecol Manag* 62:16–27. <https://doi.org/10.2111/08-100>
- Mitsch WJ, Gosselink JG (2007) *Wetlands*. Wiley, Hoboken
- Mladinich CS, Bustos MR, Stitt S et al (2006) The use of Landsat 7 enhanced thematic mapper plus for mapping leafy spurge. *Rangel Ecol Manag* 59:500–506. <https://doi.org/10.2111/06-027R1.1>
- Moisan TAH, Sathyendranath S, Bouman HA (2012) Ocean color remote sensing of phytoplankton functional types. In: Fatoyinbo L (ed) *Remote sensing of biomass-principles and applications*. InTech, Croatia. <https://doi.org/10.5772/17174>
- Mooney HA, Cleland EE (2001) The evolutionary impact of invasive species. *Proc Natl Acad Sci* 98:5446–5451. <https://doi.org/10.1073/pnas.091093398>
- Morel A, B elanger S (2006) Improved detection of turbid waters from ocean color sensors information. *Remote Sens Environ* 102:237–249. <https://doi.org/10.1016/j.rse.2006.01.022>
- Mortensen DA, Rauschert ESJ, Nord AN, Jones BP (2009) Forest roads facilitate the spread of invasive plants. *Invasive Plant Sci Manag* 2:191–199. <https://doi.org/10.1614/ipsm-08-125.1>
- Mouw CB, Hardman-Mountford NJ, Alvain S et al (2017) A consumer’s guide to satellite remote sensing of multiple phytoplankton groups in the global ocean. *Front Mar Sci* 4(41). <https://doi.org/10.3389/fmars.2017.00041>
- Muller-Karger FE, Hestir E, Ade C et al (2018) Satellite sensor requirements for monitoring essential biodiversity variables of coastal ecosystems. *Ecol Appl* 28:749–760. <https://doi.org/10.1002/eap.1682>
- Murphy BP, Andersen AN, Parr CL (2016) The underestimated biodiversity of tropical grassy biomes. *Philos Trans R Soc B Biol Sci* 371:20150319. <https://doi.org/10.1098/rstb.2015.0319>
- N asi R, Honkavaara E, Lyytik ainen-Saarenmaa P et al (2015) Using UAV-based photogrammetry and hyperspectral imaging for mapping bark beetle damage at tree-level. *Remote Sens* 7:15467–15493. <https://doi.org/10.3390/rs71115467>
- National Invasive Species Council (2016) *Management plan: 2016–2018*. NISC, Washington, D.C.
- Nelson SAC, Cheruvilil KS, Soranno PA (2006) Satellite remote sensing of freshwater macrophytes and the influence of water clarity. *Aquat Bot* 85:289–298. <https://doi.org/10.1016/j.aquabot.2006.06.003>
- Odermatt D, Gitelson A, Brando VE, Schaepman M (2012) Review of constituent retrieval in optically deep and complex waters from satellite imagery. *Remote Sens Environ* 118:116–126. <https://doi.org/10.1016/j.rse.2011.11.013>
- Olenin S, Gollasch S, Jonu sas S, Rimkut e I (2000) En-route investigations of plankton in ballast water on a ship’s voyage from the Baltic Sea to the open Atlantic coast of Europe. *Int Rev Hydrobiol*, 85:577–596. [https://doi.org/10.1002/1522-2632\(200011\)85:5/6<577::aid-iroh577>3.0.co;2-c](https://doi.org/10.1002/1522-2632(200011)85:5/6<577::aid-iroh577>3.0.co;2-c)
- Olenina I, Wasmund N, Hajdu S et al (2010) Assessing impacts of invasive phytoplankton: the Baltic Sea case. *Mar Pollut Bull* 60:1691–1700. <https://doi.org/10.1016/j.marpollbul.2010.06.046>
- Ortiz SM, Breidenbach J, K andler G (2013) Early detection of bark beetle green attack using TerraSAR-X and RapidEye data. *Remote Sens* 5:1912–1931. <https://doi.org/10.3390/rs5041912>
- Paap T, Burgess TI, Wingfield MJ (2017) Urban trees: bridge-heads for forest pest invasions and sentinels for early detection. *Biol Invasions* 19:3515–3526. <https://doi.org/10.1007/s10530-017-1595-x>
- Pearlstine L, Portier KM, Smith SE (2005) Textural discrimination of an invasive plant, *Schinus terebinthifolius*, from low altitude aerial digital imagery. *Photogramm Eng Remote Sens* 71:289–298. <https://doi.org/10.14358/PERS.71.3.289>
- Penk MR, Jeschke JM, Minchin D, Donohue I (2016) Warming can enhance invasion success through asymmetries in energetic performance. *J Anim Ecol* 85:419–426. <https://doi.org/10.1111/1365-2656.12480>
- Peterson EB (2005) Estimating cover of an invasive grass (*Bromus tectorum*) using tobit regression and phenology derived from two dates of Landsat ETM + data. *Int J Remote Sens* 26:2491–2507. <https://doi.org/10.1080/01431160500127815>
- Phinn S, Roelfsema C, Dekker A et al (2008) Mapping seagrass species, cover and biomass in shallow waters: an assessment of satellite multi-spectral and airborne hyper-spectral imaging systems

- in Moreton Bay (Australia). *Remote Sens Environ* 112:3413–3425. <https://doi.org/10.1016/j.rse.2007.09.017>
- Pimentel D, Zuniga R, Morrison D (2005) Update on the environmental and economic costs associated with alien-invasive species in the United States. *Ecol Econ* 52:273–288. <https://doi.org/10.1016/j.ecolecon.2004.10.002>
- Primack RB, Laube J, Gallinat AS, Menzel A (2015) From observations to experiments in phenology research: investigating climate change impacts on trees and shrubs using dormant twigs. *Ann Bot* 116:889–897. <https://doi.org/10.1093/aob/mcv032>
- Pu R, Gong P, Tian Y et al (2008) Using classification and NDVI differencing methods for monitoring sparse vegetation coverage: a case study of saltcedar in Nevada, USA. *Int J Remote Sens* 29:3987–4011. <https://doi.org/10.1080/01431160801908095>
- Pyšek P, Jarošík V, Pergl J et al (2009) The global invasion success of Central European plants is related to distribution characteristics in their native range and species traits. *Divers Distrib* 15:891–903. <https://doi.org/10.1111/j.1472-4642.2009.00602.x>
- Radomski P, Holbrook BV (2015) A comparison of two hydroacoustic methods for estimating submerged macrophyte distribution and abundance: a cautionary note. *J Aquat Plant Manag* 53:151–159
- Ramsey III EW, Nelson GA, Sapkota SK et al (2002) Mapping Chinese tallow with color-infrared photography. *Photogramm Eng Remote Sens* 68:251–255
- Ramsey III E, Rangoonwala A, Nelson G, Ehrlich R (2005) Mapping the invasive species, Chinese tallow, with EO1 satellite Hyperion hyperspectral image data and relating tallow occurrences to a classified Landsat Thematic Mapper land cover map. *Int J Remote Sens* 26:1637–1657. <https://doi.org/10.1080/01431160512331326701>
- Resasco J, Hale AN, Henry MC, Gorchov DL (2007) Detecting an invasive shrub in a deciduous forest understory using late-fall Landsat sensor imagery. *Int J Remote Sens* 28:3739–3745. <https://doi.org/10.1080/01431160701373721>
- Ricciardi A (2007). Are modern biological invasions an unprecedented form of global change?. *Conserv Biol* 21(2):329–336. <https://doi.org/10.1111/j.1523-1739.2006.00615.x>
- Ricciardi A, Palmer ME, Yan ND (2011) Should biological invasions be managed as natural disasters? *Bioscience* 61:312–317. <https://doi.org/10.1525/bio.2011.61.4.11>
- Rocchini D, Andreo V, Förster M et al (2015) Potential of remote sensing to predict species invasions: a modelling perspective. *Prog Phys Geogr* 39:283–309. <https://doi.org/10.1177/0309133315574659>
- Rouse JW, Benton AR, Toler RW, Haas RH (1975) Three examples of applied remote sensing of vegetation. In: *NASA earth resources survey symposium, vol 1-C*. NASA, Houston, pp 1797–1810
- Rupprecht CDD, Byrne JA, Garden JG, Hero J-M (2015) Informal urban green space: a trilingual systematic review of its role for biodiversity and trends in the literature. *Urban For Urban Green* 14:883–908. <https://doi.org/10.1016/j.ufug.2015.08.009>
- Samiappan S, Turnage G, Hathcock L et al (2017) Using unmanned aerial vehicles for high-resolution remote sensing to map invasive *Phragmites australis* in coastal wetlands. *Int J Remote Sens* 38:2199–2217. <https://doi.org/10.1080/01431161.2016.1239288>
- Santos MJ, Whitham TG (2010) Predictors of *Ips confusus* outbreaks during a record drought in Southwestern USA: implications for monitoring and management. *Environ Manag* 45:239–249. <https://doi.org/10.1007/s00267-009-9413-6>
- Santos MJ, Khanna S, Hestir EL et al (2009) Use of hyperspectral remote sensing to evaluate efficacy of aquatic plant management. *Invasive Plant Sci Manag* 2:216–229. <https://doi.org/10.1614/IPSM-08-115.1>
- Santos MJ, Hestir EL, Khanna S, Ustin SL (2012) Image spectroscopy and stable isotopes elucidate functional dissimilarity between native and nonnative plant species in the aquatic environment. *New Phytol* 193:683–695. <https://doi.org/10.1111/j.1469-8137.2011.03955.x>
- Santos MJ, Khanna S, Hestir EL et al (2016) Measuring landscape-scale spread and persistence of an invaded submerged plant community from airborne remote sensing. *Ecol Appl* 26:1733–1744. <https://doi.org/10.1890/15-0615>

- Sathyendranath S, Aiken J, Alvain S (2014) Phytoplankton functional types from space. In: Reports and monographs of the international ocean-colour coordinating group. International Ocean-Colour Coordinating Group, p 163
- Saul WC, Roy HE, Booy O et al (2017) Assessing patterns in introduction pathways of alien species by linking major invasion data bases. *J Appl Ecol* 54:657–669. <https://doi.org/10.1111/1365-2664.12819>
- Scheffer M, Szabo S, Gragnani A et al (2003) Floating plant dominance as a stable state. *Proc Natl Acad Sci U S A* 100:4040–4045. <https://doi.org/10.1073/pnas.0737918100>
- Seebens H, Blackburn TM, Dyer EE et al (2017) No saturation in the accumulation of alien species worldwide. *Nat Commun* 8:14435. <https://doi.org/10.1038/ncomms14435>
- Serrano L, Peñuelas J, Ustin SL (2002) Remote sensing of nitrogen and lignin in Mediterranean vegetation from AVIRIS data: decomposing biochemical from structural signals. *Remote Sens Environ* 81:355–364. [https://doi.org/10.1016/S0034-4257\(02\)00011-1](https://doi.org/10.1016/S0034-4257(02)00011-1)
- Shafiq B, Price WJ, Prather TS et al (2004) Using landscape characteristics as prior information for Bayesian classification of yellow starthistle. *Weed Sci* 52:948–953. <https://doi.org/10.1614/WS-04-042R1>
- Shouse M, Liang L, Fei S (2012) Identification of understory invasive exotic plants with remote sensing: in urban forests. *Int J Appl Earth Obs Geoinf* 21:525–534. <https://doi.org/10.1016/j.jag.2012.07.010>
- Simberloff D (2000) Global climate change and introduced species in United States forests. *Sci Total Environ* 262:253–261. [https://doi.org/10.1016/S0048-9697\(00\)00527-1](https://doi.org/10.1016/S0048-9697(00)00527-1)
- Sims DA, Gamon JA (2002) Relationships between leaf pigment content and spectral reflectance across a wide range of species, leaf structures and developmental stages. *Remote Sens Environ* 81:337–354. [https://doi.org/10.1016/S0034-4257\(02\)00010-X](https://doi.org/10.1016/S0034-4257(02)00010-X)
- Singh N, Glenn NF (2009) Multitemporal spectral analysis for cheatgrass (*Bromus tectorum*) classification. *Int J Remote Sens* 30:3441–3462. <https://doi.org/10.1080/01431160802562222>
- Singh KK, Davis AJ, Meentemeyer RK (2015) Detecting understory plant invasion in urban forests using LiDAR. *Int J Appl Earth Obs Geoinf* 38:267–279. <https://doi.org/10.1016/j.jag.2015.01.012>
- Soltani N, Dille JA, Burke IC et al (2016) Potential corn yield losses from weeds in North America. *Weed Technol* 30:979–984. <https://doi.org/10.1614/WT-D-16-00046.1>
- Soltani N, Dille JA, Burke IC et al (2017) Perspectives on potential soybean yield losses from weeds in North America. *Weed Technol* 31:148–154. <https://doi.org/10.1017/wet.2016.2>
- Subba Rao DV, Sprules WG, Locke A, Carlton JT (1994) Exotic phytoplankton species from ships' ballast waters: risk of potential spread to mariculture sites on Canada's east coast. *Can data Rep Fish Aquat Sci* 937:1–51
- Tabacchi E, Correll DL, Hauer R et al (1998) Development, maintenance and role of riparian vegetation in the river landscape. *Freshw Biol* 40:497–516. <https://doi.org/10.1046/j.1365-2427.1998.00381.x>
- Theoharides KA, Dukes JS (2007) Plant invasion across space and time: factors affecting nonindigenous species success during four stages of invasion. *New Phytol* 176:256–273. <https://doi.org/10.1111/j.1469-8137.2007.02207.x>
- Thornton PE, Thornton MM, Mayer BW et al (2018) Daymet: daily surface weather data on a 1-km grid for North America, Version 3. ORNL DAAC, Oak Ridge. <https://doi.org/10.3334/ORNLDAAC/1328>
- Tockner K, Malard F, Ward JV (2000) An extension of the food pulse concept. *Hydrol Process* 2883:2861–2883
- Turbelin AJ, Malamud BD, Francis RA (2017). Mapping the global state of invasive alien species: patterns of invasion and policy responses. *Global Ecol Biogeogr* 26(1):78–92. <https://doi.org/10.1111/geb.12517>
- UNESCO (2018). UNESCO'S commitment to biodiversity. In M. Bouamrane (ed.). Paris: United Nations educational, scientific and cultural organization, <https://www.unesdoc.unesco.org/images/0026/002652/265200e.pdf>

- Ustin SL, DiPietro D, Olmstead K et al (2002) Hyperspectral remote sensing for invasive species detection and mapping. *IEEE Int Geosci Remote Sens Symp* 3:1658–1660. <https://doi.org/10.1109/IGARSS.2002.1026212>
- van Kleunen M, Dawson W, Essl F et al (2015) Global exchange and accumulation of non-native plants. *Nature* 525:100–103. <https://doi.org/10.1038/nature14910>
- Venugopal G (2002) Monitoring the effects of biological control of water hyacinths using remotely sensed data: a case study of Bangalore, India. *Singap J Trop Geogr* 19:91–105. <https://doi.org/10.1111/1467-9493.00027>
- Verma R, Singh SP, Ganesha Raj K (2003) Assessment of changes in water-hyacinth coverage of water bodies in northern part of Bangalore city using temporal remote sensing data. *Curr Sci* 84:795–804
- Villa P, Mousivand A, Bresciani M (2014) Aquatic vegetation indices assessment through radiative transfer modeling and linear mixture simulation. *Int J Appl Earth Obs Geoinf* 30:113–127. <https://doi.org/10.1016/j.jag.2014.01.017>
- Villa P, Bresciani M, Bolpagni R et al (2015) A rule-based approach for mapping macrophyte communities using multi-temporal aquatic vegetation indices. *Remote Sens Environ* 171:218–233. <https://doi.org/10.1016/j.rse.2015.10.020>
- Villa P, Pinaridi M, Tóth VR et al (2017) Remote sensing of macrophyte morphological traits: implications for the management of shallow lakes. *J Limnol* 76:109–126. <https://doi.org/10.4081/jlimnol.2017.1629>
- Vis C, Hudon C, Carignan R (2003) An evaluation of approaches used to determine the distribution and biomass of emergent and submerged aquatic macrophytes over large spatial scales. *Aquat Bot* 77:187–201. [https://doi.org/10.1016/S0304-3770\(03\)00105-0](https://doi.org/10.1016/S0304-3770(03)00105-0)
- Vörösmarty C, McIntyre P, Gessner M et al (2010) Global threats to human water security and river biodiversity. *Nat Commun* 467:555–561. <https://doi.org/10.1038/nature09440>
- Walther GR, Roques A, Hulme PE et al (2009) Alien species in a warmer world: risks and opportunities. *Trends Ecol Evol* 24:686–693. <https://doi.org/10.1016/j.tree.2009.06.008>
- Ward JV, Tockner K, Arscott DB, Claret C (2002) Riverine landscape diversity. *Freshw Biol* 47:517–539. <https://doi.org/10.1046/j.1365-2427.2002.00893.x>
- Waycott M, Duarte CM, Carruthers TJB et al (2009) Accelerating loss of seagrasses across the globe threatens coastal ecosystems. *Proc Natl Acad Sci* 106:12377–12381. <https://doi.org/10.1073/pnas.0905620106>
- Weisberg PJ, Diltz TE, Baughman OW et al (2017) Development of remote sensing indicators for mapping episodic die-off of an invasive annual grass (*Bromus tectorum*) from the Landsat archive. *Ecol Indic* 79:173–181. <https://doi.org/10.1016/j.ecolind.2017.04.024>
- West AM, Evangelista PH, Jarnevich CS et al (2017) Using multi-date satellite imagery to monitor invasive grass species distribution in post-wildfire landscapes: an iterative, adaptable approach that employs open-source data and software. *Int J Appl Earth Obs Geoinf* 59:135–146. <https://doi.org/10.1016/j.jag.2017.03.009>
- Wilfong BN, Gorchov DL, Henry MC (2009) Detecting an invasive shrub in deciduous forest understories using remote sensing. *Weed Sci* 57:512–520. <https://doi.org/10.1614/WS-09-012.1>
- Williams SL, Grosholz ED (2008) The invasive species challenge in estuarine and coastal environments: marrying management and science. *Estuar Coasts* 31:3–20. <https://doi.org/10.1007/s12237-007-9031-6>
- Williams AP, Hunt ER Jr (2002) Estimation of leafy spurge cover from hyperspectral imagery using mixture tuned matched filtering. *Remote Sens Environ* 82:446–456. [https://doi.org/10.1016/S0034-4257\(02\)00061-5](https://doi.org/10.1016/S0034-4257(02)00061-5)
- Winfield IJ, Onoufriou C, O’Connell MJ et al (2007) Assessment in two shallow lakes of a hydroacoustic system for surveying aquatic macrophytes. In: Gulati RD, Lammens E, De Pauw N, Van Donk E (eds) *Hydrobiologia*. Springer Netherlands, Dordrecht, pp 111–119
- Wolf AA, Zavaleta ES, Selmants PC (2017) Flowering phenology shifts in response to biodiversity loss. *Proc Natl Acad Sci* 114:3463–3468. <https://doi.org/10.1073/pnas.1608357114>

- Wu Y, Rutchey K, Wang N, Godin J (2006) The spatial pattern and dispersion of *Lygodium microphyllum* in the Everglades wetland ecosystem. *Biol Invasions* 8:1483–1493. <https://doi.org/10.1007/s10530-005-5840-3>
- Yang C (2007) Evaluating airborne hyperspectral imagery for mapping waterhyacinth infestations. *J Appl Remote Sens* 1:013546. <https://doi.org/10.1117/1.2821827>
- Yang C, Everitt JH (2010) Comparison of hyperspectral imagery with aerial photography and multispectral imagery for mapping broom snakeweed. *Int J Remote Sens* 31:5423–5438. <https://doi.org/10.1080/01431160903369626>
- Yuan L, Zhang LQ (2008) Mapping large-scale distribution of submerged aquatic vegetation coverage using remote sensing. *Ecol Inform* 3:245–251. <https://doi.org/10.1016/j.ecoinf.2008.01.004>
- Zhao D, Jiang H, Yang T et al (2012) Remote sensing of aquatic vegetation distribution in Taihu Lake using an improved classification tree with modified thresholds. *J Environ Manag* 95:98–107. <https://doi.org/10.1016/j.jenvman.2011.10.007>

Open Access This chapter is licensed under the terms of the Creative Commons Attribution 4.0 International License (<http://creativecommons.org/licenses/by/4.0/>), which permits use, sharing, adaptation, distribution and reproduction in any medium or format, as long as you give appropriate credit to the original author(s) and the source, provide a link to the Creative Commons license and indicate if changes were made.

The images or other third party material in this chapter are included in the chapter's Creative Commons license, unless indicated otherwise in a credit line to the material. If material is not included in the chapter's Creative Commons license and your intended use is not permitted by statutory regulation or exceeds the permitted use, you will need to obtain permission directly from the copyright holder.

